

**From the Institute of Dermatology and Venerology  
of the University of Lübeck  
Director: Prof. Dr. Detlef Zillikens**

**in cooperation with  
EUROIMMUN Medizinische Labordiagnostika AG  
Head: Prof. Dr. Winfried Stöcker**

# **“Anti-neuronal autoantibodies in ischemic stroke and in anti-MAG IgM Gammopathy”**

Dissertation for the fulfillment of requirements  
for the Doctoral Degree  
of the University of Lübeck

from the Department of Natural Sciences

Submitted by

Rittika Chunder  
from Calcutta, India

Lübeck 2017

First referee: Prof. Dr. Ralf Ludwig

Second referee: Prof. Dr. Ulrich Schaible

Date of oral examination: 21.11.2017

Approved for printing: Lübeck, 28.11.2017

## **1. Abstract**

## **2. Introduction**

- 2.1 B cells and their development
- 2.2 Mature naïve B cell
- 2.3 Activation of mature naïve B cells
- 2.4 Antibodies
  - 2.4.1 Structure of an antibody
  - 2.4.2 Classes of antibodies
  - 2.4.3 Affinity and avidity of an antibody molecule
  - 2.4.4 Diversity of antibodies
- 2.5 Autoantibodies as predictors of disease
- 2.6 Central Nervous System (CNS)
- 2.7 The Blood-brain-barrier (BBB)
- 2.8 Stroke
- 2.9 Pathophysiology of ischemic stroke
- 2.10 Possible development of an autoimmune response following stroke
- 2.11 Autoantibodies in stroke
- 2.12 The Peripheral Nervous System (PNS) and the Blood-nerve-barrier (BNB)
- 2.13 Expression of peripheral nerve myelin antigens
- 2.14 Myelin associated glycoprotein (MAG)

- 2.15 Expression of immunogenic structure HNK-1
- 2.16 Paraproteinemic neuropathies (PPN)
- 2.17 Anti-MAG/HNK-1 IgM Gammopathy
- 2.18 Pathophysiology of anti-MAG IgM Gammopathy
- 2.19 Detection of anti-MAG IgM antibodies

### **3. Aims and Objectives**

### **4. Materials and Methods**

- 4.1 Buffers, media and solutions
- 4.2 Antibodies
- 4.3 Human sera
- 4.4 Indirect immunofluorescence test (IIFT)
- 4.5 DNA *in vitro* cloning and recombinant protein expression
  - 4.5.1 Expression plasmids used
  - 4.5.2 Construction of expression plasmids
  - 4.5.3 Amplification of DNA fragments by PCR
  - 4.5.4 Digestion by endonucleases
  - 4.5.5 Ligation and transformation
  - 4.5.6 Plasmid preparation and sequencing
  - 4.5.7 Generation of recombinant IIFT substrates
- 4.6 Immunoprecipitation analysis

- 4.7 Transfection of HEK293 cells for protein purification
- 4.8 Immobilized metal affinity chromatography (IMAC)
- 4.9 Ion exchange chromatography (IEX)
- 4.10 Neutralization assay
- 4.11 Biocinchoninic acid assay (BCA)
- 4.12 Enzyme linked immunosorbent assay (ELISA)

## **5. Results**

- 5.1 Stroke does not induce autoantibodies against neuronal structures
  - 5.1.1 Analysis for IgG response
  - 5.1.2 Analysis for IgM response
  - 5.1.3 Analysis for IgA response
- 5.2 Cloning of MAG/ MAG(ec), GlcAT, HNK-1ST and GlcAT [E284A]
- 5.3 Generation of HNK-1 target antigen by recombinant techniques
- 5.4 Antibody binding to HNK-1 target antigen in HEK293 cells is GlcAT-P dependent
- 5.5 Generation of GlcAT-P [E284A] mutant transfected HEK293 cells
- 5.6 Confirmation of HNK-1 glycosylation of MAG and MAG(ec)-H6 in HEK293 cells
- 5.7 IMAC purification of the His-tagged soluble extracellular domain of MAG
- 5.8 No neutralization of anti-HNK-1 IgM antibody by soluble glycosylated MAG

5.9 Sequencing of variable heavy (VH) and variable light (VL) of anti-HNK-1 mouse IgM Hybridoma

5.10 Anti-MAG/HNK-1 IgM ELISA

## **6. Discussion**

6.1 Ischemic stroke does not result in the induction of new autoantibodies against neuronal structures

6.2 Development of new diagnostic tools for the detection of anti-MAG/HNK-1 IgM antibodies

6.3 Concluding remarks

## **7. Bibliography**

List of figures

List of tables

List of abbreviations

Acknowledgement

# 1. Abstract

## Summary

Neuroinflammatory disorders involve immune mediated damage of the central nervous system (CNS) and peripheral nervous system (PNS) resulting in both physical and emotional disability of the affected individuals. Typical examples of neuroinflammation display a complex interaction between the cellular and humoral components of the immune system with the nervous system parenchyma.

In the present work a systematic search for stroke induced autoantibodies that target neuronal structures has been performed based on indirect immunofluorescence assays validated for diagnostic purposes. There were no indications of anti-neuronal autoantibody induction following stroke. These results are in line with the stroke-induced immunosuppression phenomenon described by others. Positive findings of stroke induced autoantibody formation by other groups are mainly based on *in house* assays not validated for diagnostic purposes. This might explain the controversial findings and highlights the need to use well validated diagnostic assays; preferably a combination of tissue and recombinant cell based substrates for indirect immunofluorescence test (IIFT).

Anti-MAG IgM Gammopathy is a paraproteinemia characterized by antibodies that bind to MAG and other structures expressing the human natural killer 1 (HNK-1) glycoepitope. Diagnosis of the disease is supported by the identification of these antibodies. Tissue based IIFT on sections of peripheral nerve have proven to be very useful. Employing recombinant techniques a new MAG-HNK-1 substrate for IIFT has been developed that is characterized by superior sensitivity and specificity and might replace the tissue based substrate. To further improve the accuracy of antibody quantification, an ELISA based on soluble HNK-1 modified MAG has been developed and functionally validated. To standardize these assays a chimeric mouse/human IgM with specificity to the HNK-1

glycoepitope has also been generated based on the mouse IgM Hybridoma TIB-200 that proves to bind to HNK-1 modified structures.



## Zusammenfassung

Neuroinflammatorische Erkrankungen sind mit immunvermittelten Schäden des zentralen Nervensystems (ZNS) und des peripheren Nervensystems (PNS) verbunden. Das führt zu sowohl physischer als auch emotionaler Beeinträchtigung der betroffenen Personen. Typische Beispiel von Neuroinflammation zeigen eine komplexe Interaktion zwischen den zellulären und humoralen Bestandteilen des Immunsystems mit dem Parenchyms des Nervensystems.

Im Zuge der vorliegenden Arbeit wurde eine systematische Suche nach Schlaganfall-induzierten Autoantikörpern durchgeführt, die gegen neuronale Strukturen gerichtet sind. Dies geschah auf der Basis von indirekten Immunfluoreszenz-Tests (IIFT) für diagnostische Anwendungen. Es wurden keine Anzeichen für das Entstehen antineuronaler Antikörper nach einem Schlaganfall gefunden. Diese Ergebnisse stehen im Einklang mit dem Schlaganfall-induzierten Immunsuppressionsphänomen, das in anderen Arbeiten beschrieben wurde. Positive Funde einer Schlaganfall-induzierten Antikörperbildung durch andere Gruppen basierten zumeist auf innerbetrieblichen Tests, die nicht für diagnostische Zwecke validiert waren. Dies könnte die kontroversen Ergebniss erklären und verdeutlicht die die Notwendigkeit für gut validierte diagnostische Tests, vorzugweise auf der Basis einer Kombination aus gewebebasierten und zellbasierten Substraten für den IIFT.

Die Anti-MAG-IgM-Gammopathie ist eine Paraproteinämie, die durch Antikörper gekennzeichnet ist, die an MAG und andere Strukturen binden, welche das *human natural killer 1* (HNK-1) Glykoepitop tragen. Die Diagnose dieser Erkrankung stützt sich auf die Identifikation dieser Antikörper. Ein IIFT basierend auf Gewebeschnitten peripherer Nerven hat sich als sehr nützlich erwiesen. Durch die Verwendung von Rekombinationstechniken wurde ein neues MAG-HNK-1-Substrat entwickelt, das sich durch ausgezeichnete Sensitivität und Spezifität auszeichnet und die gewebebasierten Substrate ersetzen könnte.

Um die Genauigkeit der Antikörper-Quantifizierung weiter zu verbessern, wurde

ein ELISA basierend auf löslichem HNK-1-modifizierten MAG entwickelt und funktionell validiert. Um diesen Test zu standardisieren wurde auch ein chimärer muriner/humaner IgM mit Spezifität zum HNK-1-Glykoepitop generiert, basierend auf dem murinen IgM-Hybridom TIB-200, das nachgewiesenermaßen an HNK-1-modifizierte Strukturen bindet.

## **2. Introduction**

### **2.1 B cells and their development**

B cells are a subset of lymphocytes of the adaptive immune system that express clonally diverse antigen recognition molecules known as immunoglobulins (Ig). Membrane-bound Ig on the surface of B cells act as receptors, known as B cell receptors (BCR), that recognize specific antigenic epitopes.

The development and differentiation of a B cell begins in the bone marrow from a pro-B cell to an immature naïve B cell.<sup>1,2</sup> At this stage of development, B cells undergo various checkpoints, like clonal deletion and receptor editing, which prevents the development of self-reactive cells. Clonal deletion is a process by which the immature B cell in the bone marrow undergoes apoptotic death as a consequence of recognizing a self antigen. Whereas, receptor editing can be defined as the modification of an undesired BCR, either non-functional or of autoreactive specificities, with a BCR which has more acceptable characteristics.<sup>3,4,5</sup> B cells that successfully complete this checkpoint leave the bone marrow as transitional B cells.<sup>6</sup> Nonetheless, these checkpoints are generally imperfect, and B cells capable of self-directed autoimmune responses are common and a part of the healthy immune repertoire.<sup>7,8</sup>

### **2.2 Mature naïve B cell**

A mature naïve B cell can generally be divided into three further subsets, B1 B cells, marginal zone (MZ) B cells and follicular B cells.<sup>9</sup> B1 cells are a self-renewing B cell population that function independently of CD4+ T helper cells and provide adaptive immune response to T cell independent antigens like polysaccharides and other carbohydrate structures.<sup>10</sup> MZ B cells are considered to be innate-like cells that may be involved in the transport of antigens in immune complexes in the secondary lymphoid organs.<sup>11</sup> Follicular B cells, which constitute the majority of mature B cells, populate the B cell follicles in lymph nodes and the spleen, recirculating in the blood and require cognate help from CD4+ T cells.<sup>12</sup>

## **2.3 Activation of mature naïve B cells**

When mature naïve B cells encounter their cognate antigen in the secondary lymphoid tissue, they become activated. While the primary signal for B cell activation is this binding of antigen to the antigen-specific receptor expressed by the B cell, in most cases subsequent secondary signals are also required. This second signal is often provided by the interaction of the B cell with antigen-specific CD4+ helper T cells.<sup>13,14</sup> Following activation, some of these B cells – in conjunction with CD4+ T cell help – take part in germinal center (GC) reactions within the lymphoid follicles. Lymphoid follicles in secondary lymphoid tissue have a complex microenvironment comprising of immune cells, adhesion molecules and antigen-antibody complexes and act as a site of antigen-induced B cell proliferation. Whereas, GCs are specialized areas within these lymphoid follicles where B cells undergo hypermutation leading to affinity maturation to eventually develop into memory B cells or antibody secreting plasma cells.<sup>13,15</sup> However, in some cases – mostly for antigens like polysaccharides – CD4+ T cell help is not necessary to activate mature naïve B cells. These antigens with repetitive epitopes possess an intrinsic ability to directly stimulate B cells. When a B cell encounters such an antigen with spatial co-localization of the same epitope, a strong signaling response within the cell is induced that is sufficient to generate an antibody response. Generally speaking, when a B-cell response does not require CD4+ T cell help to T-cell independent antigens, such activated B cells also do not undergo affinity maturation and are weighted more towards the production of the IgM class of antibody (Chaper 2.4).<sup>16</sup>

## **2.4 Antibodies**

Antibodies are glycoproteins that are the main effector molecules of terminally differentiated B cells secreted in response to an immunogen. They have the same unique antigen-binding sites as the cell-surface Ig that earlier served as the membrane-bound BCR.<sup>17</sup>

### **2.4.1 Structure of an antibody**

Two identical light (L) and heavy (H) polypeptide chains stabilized by disulfide bonds make up the basic structural unit of an antibody molecule. Both the light and heavy chains can further be divided into a constant (C) region at their C-terminal end and a variable (V) region at their N-terminal end.

The variable regions of heavy chains (VH) is about 110 amino acids long whereas the constant region (CH) is about three to four times longer, resulting in three or four constant domains. However, in case of the light chains, both the constant region (CL) as well as the variable region (VL) are of the same size of approximately 110 amino acids. The variation in the amino acid sequence in the variable domains of both the light and heavy chains is mostly confined to several small hypervariable regions. The hypervariable regions of the light and heavy chain variable domains form the antigen-binding site of the antibody molecule and is crucial to the diversity of antigen specificities. Further, in any given antibody molecule, the constant region gives the antibody its effector function such as complement activation, whereas the heavy-chain class determines the isotype of the antibody.<sup>18</sup>

### **2.4.2 Classes of antibodies**

The five antibody classes are IgG, IgM, IgA, IgE and IgD.

IgG is the most abundant isotype of antibody found in the body having a molecular weight of approximately 150 kDa. Each IgG molecule consists of two heavy and light chains of approximately 50 kDa and 25 kDa size. An IgG molecule can further be divided into four subclasses based on their structural, antigenic and functional differences.

IgM is always the first class of antibody that is expressed by a developing B cell. Naïve B cells express monomeric IgM on their surface while matured B cells after antigenic stimulation secrete pentameric IgM where single IgM units are linked together by disulfide bonds. The variable regions of an IgM molecule do not undergo much somatic hypermutation in response to an antigen given that IgM is

expressed early in B cell development. Therefore, IgM antibodies tend to be more polyreactive in comparison to affinity matured highly specific IgG molecules. Low-affinity IgM antibodies are also a part of the normal immune repertoire called as natural antibodies. These natural antibodies play an important role in immunoregulation.<sup>3,17</sup>

IgA are the major class of antibody present in mucosal surfaces and secretions of most mammals and act as a first line of defense against ingested or inhaled pathogens at mucosal surfaces. An IgA molecule can be divided into two subclasses.

IgE is associated with hypersensitivity and allergic reactions and are present at very low concentration in the serum.

Circulating IgD molecule is not known to participate in major antibody effector mechanisms and are found at the lowest concentration in the serum.

A general comparison between IgG and IgM is given in Table 1.

**Table 1: Summary of differences between IgG and IgM.**

<b>Class</b>	<b>IgG</b>	<b>IgM</b>
Form	Monomer	Pentamer (but expressed on the plasma membrane of B cells as a monomer)
Percentage of total immunoglobulin	Constitutes approximately 75 % of the total serum immunoglobulin	10 % of normal human serum immunoglobulin
Subclasses	4	-
Characteristic	Secondary immune response	Primary immune response

### **2.4.3 Affinity and avidity of an antibody molecule**

The binding strength of a single antigen-binding site (paratope) to a single antigenic determinant (epitope) is defined as the affinity of an antibody molecule. The total binding strength of a polyvalent antibody with its corresponding polyvalent antigen is the avidity of the interaction. While the affinity of an antibody is independent of their number of binding sites, the avidity is proportional to the

valency of the antibody. For instance, if an IgG and IgM molecule has the same affinity to a particular antigen, the IgM molecule (with 10 binding sites) will have a higher avidity than the IgG (with 2 binding sites). This property of high avidity of an IgM molecule is important in the immune response where an IgM molecule normally displays a low affinity to a given antigen.

#### 2.4.4 Diversity of antibodies

Three pools of gene segments and exons encode for an immunoglobulin molecule. One encodes for heavy chains, one pool each encodes for the two different light chains. Further, the light chain pools contain one or more C region exons and variable (V) and joining (J) gene segments while the heavy-chain pool contains sets of C-region exons and sets of V, J and diversity (D) gene segments. By random combination of inherited gene segments that code for the VL and VH regions, the immune system can make hundreds of different light chains and even a greater diversity of different heavy chains. As there are multiple genes for every gene and any of these genes can combine into an immunoglobulin variable domain, the resulting repertoire of the V domain is extraordinarily diverse. Other mechanisms contributing to the variable domain diversity include trimming or random addition of nucleotides at rearranging junctions of the V, D and J genes, as well as somatic mutations that also occur at the V domains.<sup>17,19</sup>

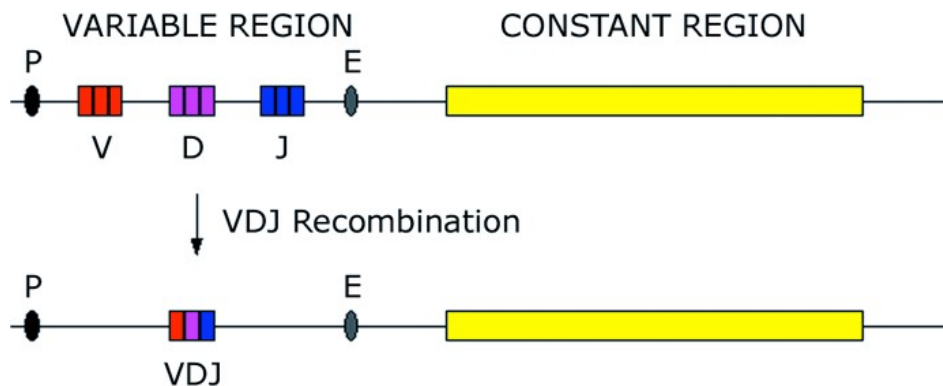


Figure 1: V(D)J recombination within a B-cell receptor. Scheme of a receptor locus where P is indicated as promoter region and E as enhancer. Adapted from Market et al., 2003.<sup>20</sup>

## **2.5 Autoantibodies as predictors of disease**

Autoantibodies, by definition, are antibodies that are directed against an individual's self components. Such autoantibodies are often a part of an autoimmune disease process, allowing them to be predictive markers of the disease activity. In some cases autoantibodies can predict the likelihood of a clinical disease as well as the rate of progression while in other cases their significance is unknown or their presence is debatable.<sup>21,22</sup>

For instance, in diseases like Neuromyelitis Optica or autoimmune encephalitis, autoantibodies are diagnostic markers to define the disease or in the case of rheumatic diseases, the corresponding autoantibody detection is used to confirm diagnosis or even predict prognosis. At the other end of the spectrum are diseases like Multiple Sclerosis where the presence of autoantibodies or their significance in mediating disease pathogenesis is debatable.<sup>23</sup>

Nonetheless, identification of disease relevant autoantibodies as biomarkers allows accurate diagnosis and designing of more specific therapies. Examples of methods used to detect such autoantibodies include Indirect immunohistochemistry and immunofluorescence, immunoblotting, radioimmunoassays and enzyme linked immunosorbent assay (ELISA).<sup>24,25</sup>

## **2.6 Central Nervous System (CNS)**

The CNS includes the brain (cerebral hemispheres, diencephalon, cerebellum, and brainstem) and the spinal cord. The meninges, which enclose and protect the CNS, are comprised of three membranes. The outermost tough fibrous membrane is the dura mater, beneath the inner surface of the skull. The arachnoid lies under the dura and the pia mater covers the CNS parenchyma. The subarachnoid space (SAS), which lies between the arachnoid and the pia mater is filled by the cerebrospinal fluid (CSF).

## **2.7 The Blood-brain-barrier (BBB)**



Large cerebral arteries enter the CNS and branch into smaller arteries and arterioles and then further into capillaries and postcapillary venules. The blood-brain-barrier (BBB) is present at this level of capillaries and postcapillary venules, consisting of highly specialized endothelial cells surrounded by pericytes, which replace the layers of smooth muscle cells in the larger arterial vessels. The tightly regulated BBB can be defined by a set of characteristics including the presence of a complex network of tight junctions (TJs).<sup>26</sup> The TJs localized at the CNS endothelium include transmembrane proteins like occludin, claudin-3, -5 and -12, cytoplasmic scaffolding proteins like Zonula occludens (ZO) -1 and ZO-2 and junctional adhesion molecules (JAM) A, JAM B and JAM C.<sup>27</sup>

The BBB thus acts as a “fence” allowing only limited movement of small lipophilic molecules from the blood to enter the brain.<sup>28,29</sup> Only defined immune cells that hold specific molecular keys to breach the BBB are allowed to enter the CNS. Further, at the abluminal side of the CNS parenchymal microvessels, there is an additional ensheathed layer of astrocytic endfeet, the glia limitans perivascularis, which acts as a mechanical barrier in addition to the BBB. The glia limitans is unique to the BBB within the CNS parenchyma.

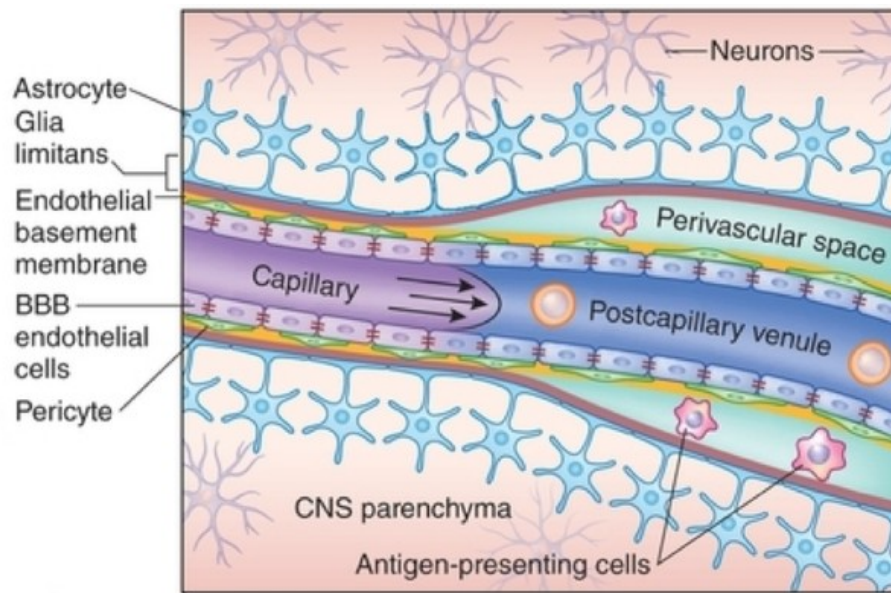


**Figure 2:** The blood–brain barrier. The BBB is localized at the level of capillaries and postcapillary venules. While transport of solutes into the CNS is controlled at the capillary BBB, trafficking of immune cells preferentially take place at the postcapillary venules. Pericytes are surrounding the

highly specialized endothelial cells. Also surrounding the CNS parenchymal microvessels is the glia limitans which is composed of astrocyte end-feet. Occasional antigen presenting cells (APCs) are seen at the perivascular space formed by the separation of the endothelial and parenchymal basement membranes at the postcapillary venules. *Adapted from Engelhardt et al., 2017.*<sup>30</sup>

## **2.8 Stroke**

Stroke, sometimes also referred to as cerebrovascular insult (CVI), has not only been reported to be the third major cause of death worldwide but it is also one of the major causes leading to long-term disability among adults.<sup>31</sup> Stroke is geographically heterogenous with the conventional risk factors including hypertension, diabetes and arteriosclerosis or a history of cardiovascular disease.

Some of the early clinical manifestations of stroke include sudden weakness of the limbs or facial muscles, difficulty in speaking or understanding of speech, unexplained dizziness or loss of balance. Stroke can be broadly classified into ischemic and hemorrhagic with ischemic stroke being the most common of these two types, accounting for ~83 % of all cases.<sup>32</sup>

## **2.9 Pathophysiology of ischemic stroke**

A number of different mechanisms are involved in and influence the pathogenesis of ischemic stroke from progression to recovery.<sup>33</sup> Mounting evidence suggests a complex crosstalk between the CNS and the immune system that plays a key role in mediating brain injury following cerebral ischemia.<sup>34</sup>

Brain tissue has a high consumption of oxygen and glucose. When there is an interruption of cerebral blood flow, the brain cells are deprived of oxygen and nutrients that are required to support metabolism of the brain. Therefore, tissue damage in response to stroke depends partly on the severity of the ischemia which in turn is dependent on the type of occlusion – whether permanent or temporary. Severe ischemia develops in the tissue immediately surrounding the occluded vessel which is the “core” area. The lesser ischemic region develops around the “core”, and is termed as the “penumbra”.<sup>35</sup> Furthermore, the ischemic cascade includes oxidative stress, excitotoxicity, apoptosis and cell death. These

processes consequently could trigger an immune response leading to neuroinflammation.<sup>33</sup> The inflammatory mechanisms involved in the pathophysiology of stroke range from exposure of molecules released by dying cells to immune cells infiltrating the site of injury/infarct. Cerebral ischemia is therefore a combination of aspects of the innate immune system as well as those of adaptive immunity, which are usually observed in autoimmune diseases of the CNS.<sup>36</sup>

## **2.10 Possible development of an autoimmune response following stroke**

Secretion of many different inflammatory cytokines and chemokines by the ischemic brain leads to an upregulation of adhesion molecules in the cerebral vasculature allowing the recruitment of peripheral lymphocytes into the brain. Activated inflammatory cells can release a variety of cytotoxic agents including matrix metalloproteinases (MMPs). MMPs not only induce further cell damage but are also instrumental in mediating disruption of the BBB which can further potentiate brain tissue injury by allowing uninhibited entry of serum elements and recruitment of immune cells from the periphery.<sup>33,37</sup>

A compromised BBB also allow antigens that are unique to the CNS – for instance, intracellular or cryptic antigens from injured neurons and glial cells – to be “released” into the periphery. It is possible that these CNS specific antigens contain epitopes which were previously “hidden” from the immune system and T- and B lymphocytes have not been tolerized towards such CNS-restricted autoantigens.<sup>38</sup> These cryptic brain antigens may be presented to patrolling autoreactive T lymphocytes by antigen presenting cells (APCs) in the peripheral lymph nodes or in the brain.<sup>39,34</sup> Alternatively, it may also be possible that these cryptic epitopes may activate cross-reactive T cells as a result of molecular mimicry.<sup>40,41</sup> T cells can subsequently also activate mature self-reacting B cells allowing them to proliferate and produce antibodies.<sup>41</sup> Therefore, following an ischemic attack the possibility of an autoimmune response to previously

sequestered brain antigens exists, where unique CNS antigens are encountered by the immune system.<sup>42,38</sup>

To summarize, the involvement of adaptive immunity in cerebral ischemia is indisputable. However, whether it plays a role in inducing a classical autoimmune response or a regulatory immune response is still debated.

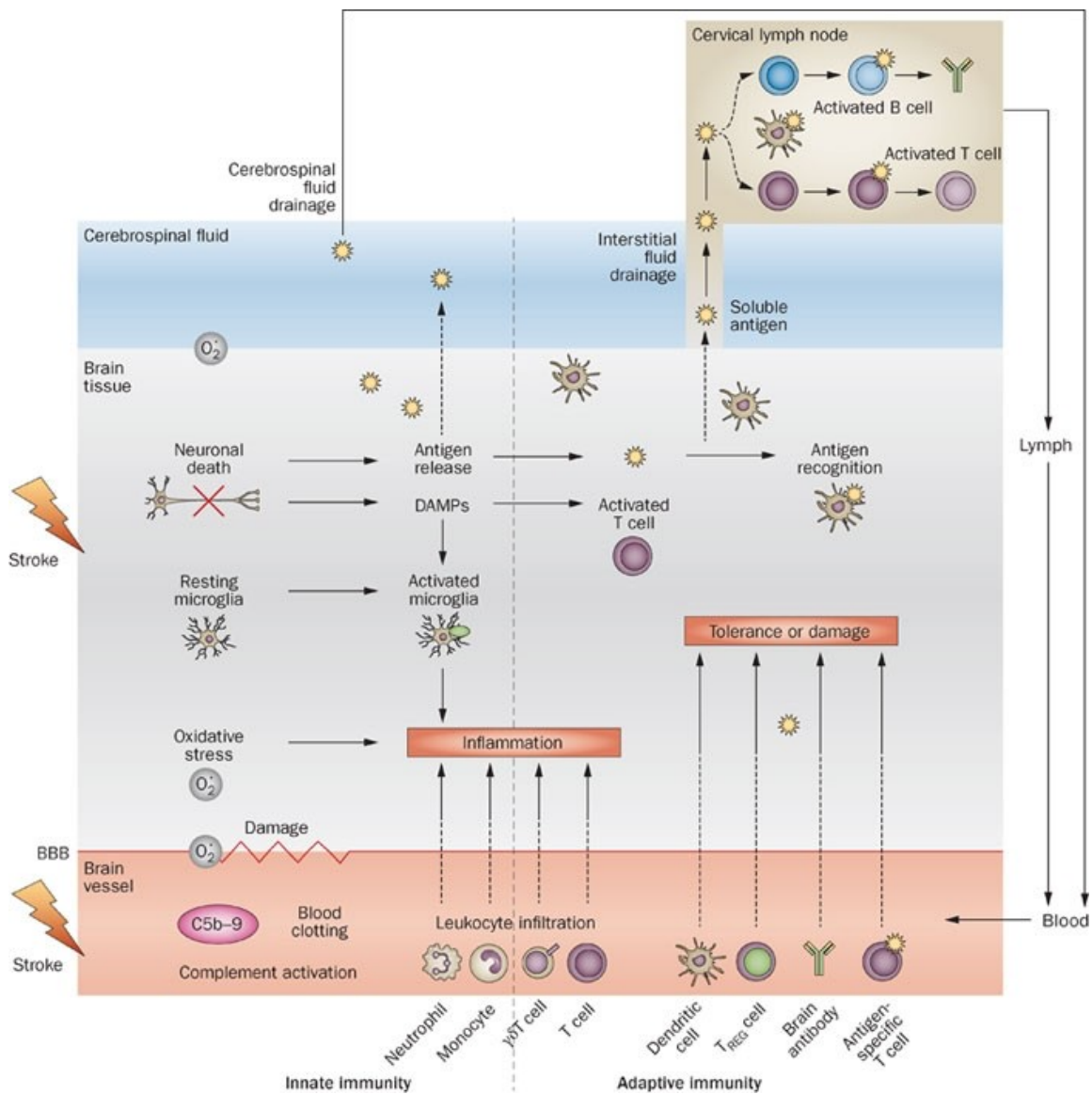


**Figure 3: Immunology of a stroke response.** A complex cascade of events is triggered following brain ischemia including oxidative stress, microglial activation and cellular infiltration of immune cells from the periphery into the ischemic CNS. Ischemic cell death results in the release of DAMPs that activate pattern recognition receptors expressed by immune cells. Release of brain antigens

that drain into the peripheral lymph nodes coupled with a compromised brain barrier, allows cells of the adaptive immune system to be activated and enter into the brain. Cytokine production and complement activation resulting from these events further aggravate tissue damage. *Adapted from Chamorro et al., 2012.*<sup>43</sup>

## 2.11 Autoantibodies in stroke

Antibodies to myelin basic protein (MBP), neuron specific enolase (NSE), glial fibrillary acidic protein (GFAP), S-100  $\beta$  and N-methyl-D-aspartate receptor (NMDAR) have been detected in the circulation after stroke demonstrated by several studies using different methods.<sup>44–46</sup>

Data from the literature proposes the presence of antibodies to neurofilaments, which are a major component of the neuronal cytoskeleton and myelin antigens in stroke patients. Studies have characterized a humoral immune response and elevated antibody titres to MBP and proteolipid protein (PLP), two of the most common myelin proteins.<sup>47,48</sup> The presence of antibodies to the myelin basic protein – among others – have been investigated as a low predictive marker that reflects the severity of a stroke.<sup>49</sup> A similar study demonstrated that autoantibodies to neurofilaments (NF) also rise within the first three months following stroke.<sup>50</sup>

Antiphospholipid antibodies (APLAs) are a group of antibodies against phospholipids and phospholipidprotein complexes. A relationship between the presence of anti-phospholipid antibodies and the risk of suffering a stroke has been suggested.<sup>51,52</sup> Studies have reported the presence of APLAs in up to 20 % of younger stroke patients under the age of 50.<sup>50,53</sup> Suggestions have been made that the presence of anticardiolipin antibodies (aCL), an important sub-type of APLAs, may be a risk factor for cerebral ischemia in the younger group of stroke patients.

NMDAR is highly expressed in the cerebral cortex and plays a crucial role in neuronal connectivity and survival. One of the studies conducted has shown that patients can develop autoantibodies to the GluN1 subunit of NMDAR after cerebral ischemia and that this is associated with worse clinical outcome, for instance, a larger infarct size.<sup>54</sup> Another study based on a peptide ELISA was

able to detect the presence of the autoantibodies to NR2A/2B subtype of NMDAR in patients with cerebral ischemia.<sup>44</sup>

However, whether these results fit to autoantibodies detectable using tissue based immunofluorescence and recombinant cell based assays is still not known.

## **2.12 The peripheral nervous system (PNS) and the blood nerve barrier (BNB)**

The peripheral nervous system is composed of the cranial nerves (except the optic nerve), nerve roots, plexuses and peripheral nerve branches including the peripheral axons and ganglia of the autonomic nervous system. Like the CNS, it also has its own barrier to the blood system, the blood-nerve-barrier (BNB). The BNB is considered to be more permeable than the blood-brain barrier since, for instance, it lacks the additional functional barrier formed by the glial limitans in the CNS (Chapter 2.7).

The major structural element of the blood-nerve-barrier is the presence of TJ proteins between endoneurial capillary endothelial cells and the perineurial cells that ensheath individual nerve fascicles. The blood-nerve-barrier also acts as an interface which actively participates in the exchange of materials between the endoneurial microenvironment and the surrounding extracellular space. Cellular and humoral immune response can successfully target PNS antigens despite the presence of the barrier.<sup>55</sup>

Pathological breakdown of the endoneurial BNB maybe a key event in the induction of various peripheral neuropathies allowing uninhibited movement of pathogenic lymphocytes and immunoglobulins into the PNS. Microvessels in some areas of the PNS, including dorsal root ganglia and nearby spinal roots, are devoid of the barrier properties and are considered to be especially vulnerable to inflammatory neuropathies.<sup>56</sup> Some immune neuropathies may be mediated directly by production of autoantibodies that are able to cross a permeable BNB.

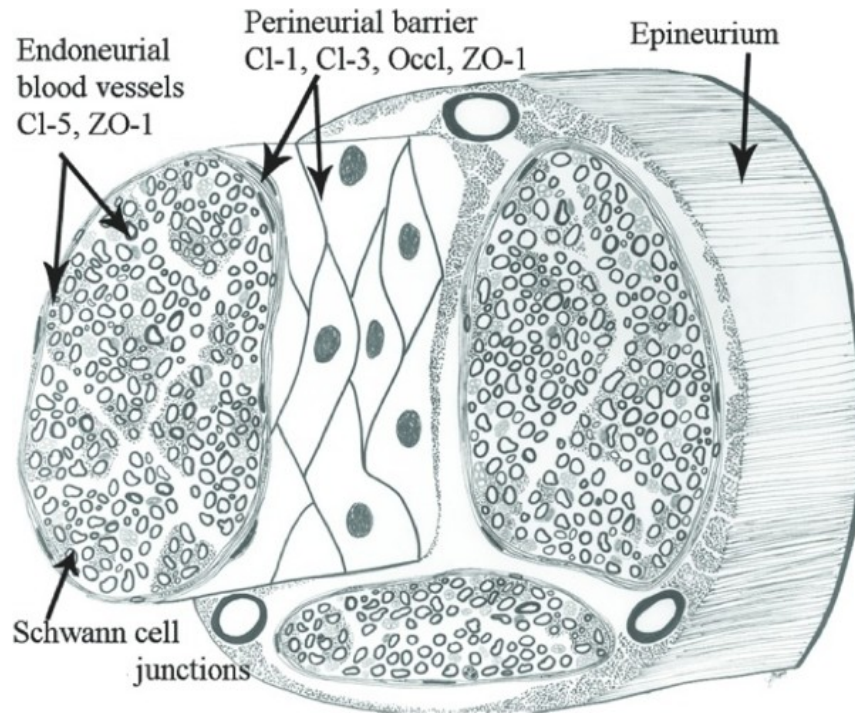


**Figure 4: The anatomical compartments of a peripheral nerve. Epineurium, perineurium and endoneurium are the three collagen-based connective tissue compartments of the peripheral nerve. The blood-nerve barrier is located in the endoneurial vasculature, where sheets of cells are held together by tight junction proteins (claudins and occludins) contributing to the barrier properties. The perineurial cells of the perineurium express tight junction proteins like occludin and claudin-1 and claudin-3 thereby forming a selective diffusion barrier between the endoneurium and epineurium. *Modified from Peltonen et al., 2013.*<sup>57</sup>**

### **2.13 Expression of peripheral nerve myelin antigens**

The myelin sheath in the PNS is a specialized extension of the plasma membrane of Schwann cells that facilitates rapid saltatory conduction of action potential. It is composed of both compact and non-compact myelin components, each of which has distinct biological functions and molecular structures.<sup>58</sup> Compact myelin forms the vast majority of the PNS myelin and includes MBP, Myelin Protein Zero (M<sub>0</sub>) and Peripheral Myelin Protein-22 (PMP-22) as the dominant proteins. Non-compact myelin which is localized at the paranodal regions includes Myelin associated glycoprotein (MAG) and Connexin 32 as well as large amounts of gangliosides, glycosphingolipids of the plasma membrane.<sup>55</sup>

### **2.14 Myelin associated glycoprotein (MAG)**

MAG is a 100 kDa type I transmembrane glycoprotein selectively localized in the periaxonal Schwann cells and oligodendroglial membranes of the PNS and CNS myelin sheaths respectively. Although a quantitatively minor component of isolated myelin, MAG is important for the formation and maintenance of myelinated axons. The periaxonal localization of MAG suggests that it could play a role in glia-axon interactions. Posttranslationally modified MAG contains about 30 % carbohydrate by weight with N-linked oligosaccharides at eight extracellular sites, most of them carrying a negative charge because of sialic acid or a sulfate group.<sup>59</sup> Human MAG displays a terminal sulfated glucuronic acid containing glycoepitope, human natural killer-1 (HNK-1). However, HNK-1 is not exclusively expressed on MAG but also on other glycoproteins and glycolipids. This HNK-1 carbohydrate epitope involving a sulfated glucuronic acid is crucial for and contributes to the antigenic properties of these proteins, including MAG.<sup>60</sup>

### **2.15 Expression of the immunogenic structure HNK-1**

The HNK-1 glycoepitope is believed to be involved in cell-cell interaction and adhesion. The characteristic structural feature of the HNK-1 carbohydrate epitope is the sulfated glucuronyl residue. The synthesis of HNK-1 is initiated by the enzymatic addition of  $\beta$ -1,3-linked glucuronic acid to N-acetyllactosamine by  $\beta$ -1,3-glucuronyltransferase (GlcAT-P), followed by the addition of the terminal sulfate group with the aid of HNK-1 sulfotransferase (HNK-1ST).<sup>61,62</sup>

In general, glycosyltransferases exhibit strict acceptor specificity. In the case of GlcAT-P, it is highly specific for the terminal N-acetyllactosamine structure.<sup>63</sup> The primary structure of the enzyme GlcAT-P is predicted to be a type II transmembrane protein of 334 amino acids and with no detectable similarities to any other protein of known function.

A soluble, active recombinant form of the enzyme GlcAT-P has previously been expressed in COS-1 cells. Transfection of the glucuronyltransferase cDNA alone into COS-1 cells induced the expression of the HNK-1 epitope on the cell surface. It was concluded from the study that COS-1 cells contain the additional enzyme, HNK-1ST, that transfers sulfate to glycoconjugates to complete the



HNK-1 epitope. Evidence also suggested that the presence of HNK-1ST might be widely distributed in various types of cells.<sup>64</sup>

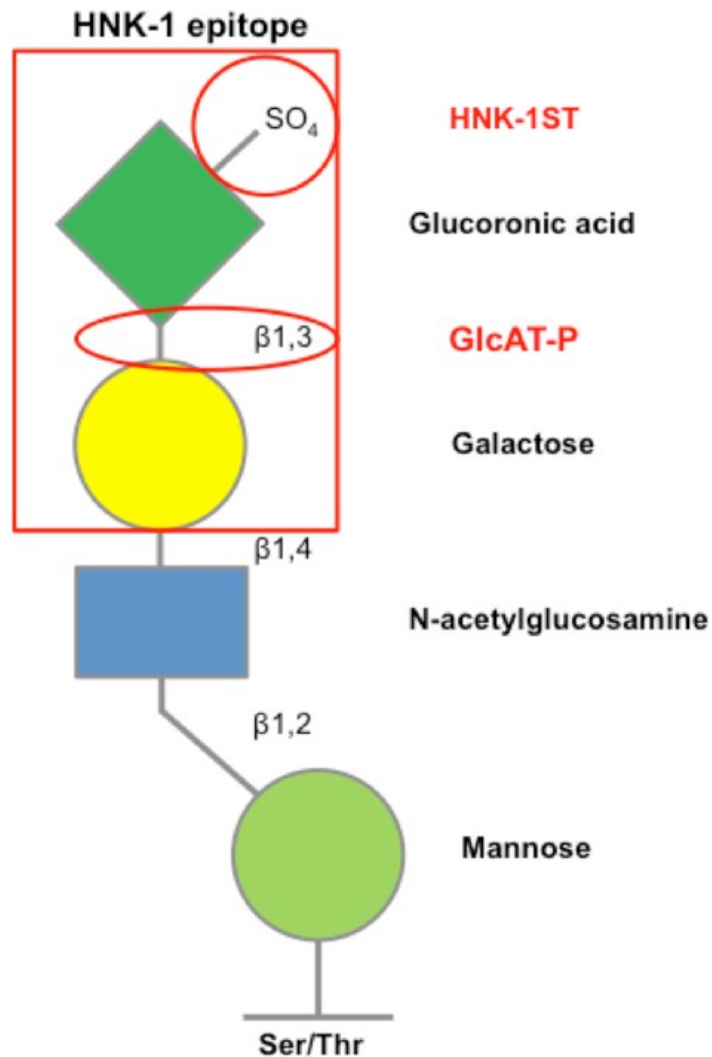


Figure 5: Formation of the HNK-1 glycoepitope. This cartoon describes the formation of an O-linked HNK-1 glycan chain, with a terminal sulfate group attached to a glucuronic acid residue. The two key enzymes involved in the formation of this glycoepitope have been indicated as GlcAT-P (glucuronyl transferase) and HNK-1ST (sulfotransferase). *Modified from Dwyer et al., 2012*<sup>65</sup>

## 2.16 Paraproteinemic neuropathies (PPN)

Paraproteinemic neuropathies describe a heterogeneous group of neuropathies characterized by the presence of excess amount of homogenous immunoglobulin in the serum. The anomalous immunoglobulins are normally monoclonal resulting from an abnormal proliferation of a single clone of B cells. Several of these

monoclonal antibody producing conditions are associated with the peripheral nervous system where antibodies interact with their specific antigenic targets on the peripheral nerves.<sup>66</sup> Although these monoclonal proteins may exist as IgG, IgM, IgA and less commonly as IgE, peripheral neuropathies are most commonly observed as IgM gammopathy (48 %), followed by IgG (37 %), and IgA (15 %). Sometimes, the monoclonal paraprotein can be a result of a malignant plasma cell or lymphoproliferative disorder. Examples of such malignant lymphoproliferative disorders associated with the PNS include multiple myeloma, primary amyloidosis and chronic lymphocytic leukemia. However, in most cases the monoclonal gammopathy is not associated with malignant clonal B cell expansion and are termed as monoclonal gammopathy of undetermined significance (MGUS). Diagnosis of blood samples by serum protein electrophoresis indicates elevated levels of immunoglobulin, while immunofixation is another method that allows discrimination between plasma cell malignancy and MGUS.

One example of a peripheral neuropathy associated with a benign monoclonal paraproteinemia is the anti-MAG IgM Gammopathy which may be described as a sensory and motor neuropathy.

### **2.17 Anti-MAG/HNK-1 IgM Gammopathy**

Anti-MAG Gammopathy is associated with the overproduction of monoclonal IgM capable to bind the glycoepitope HNK-1 present on MAG.<sup>67</sup> Since HNK-1 is also present on other sulfated glycolipids and proteins such as P0, PMP-22, phosphacan and glycosphingolipids, such glycoconjugates other than MAG can be recognized or targeted by anti-MAG IgM antibodies as long as they bear the HNK-1 glycosylation.<sup>55,68,69</sup>

Clinically, anti-MAG paraproteinemic neuropathy is a chronic and slowly progressive sensory dominant demyelinating neuropathy with a late onset with upper limb tremor being a characteristic feature of this disease.<sup>70</sup> Most patients develop sensory ataxia along with muscle weakness of various degree in addition to tremors in the extremities which increases with disease progression.<sup>71</sup>

Interestingly, although both MAG and the HNK-1 antigen are distributed in both the CNS and the PNS, anti-MAG IgM preferentially target peripheral MAG. Patients with anti-MAG IgM Gammopathy who exhibit clinical symptoms involving the CNS are extremely rare. A few isolated studies have revealed that only a subset of these patients display demyelinating lesions in the cerebral white matter. It can be speculated that due to its large pentameric configuration, IgM does not normally cross into the CNS but perhaps a continuous presence of pathogenic IgM over time may lead to a breakdown of the BBB and subsequent damage of the CNS in very few patients.<sup>72,73</sup>

Current therapeutic options available to treat these patients include intravenous immunoglobulin infusion, plasma exchange and Rituximab therapies that have been proven to be beneficial in some patients.<sup>68</sup> However, more recent demonstration of efficient removal of anti-MAG IgM antibodies using a glycopolymer represents a step towards antigen-specific therapy in these patients.<sup>74</sup>

## **2.18 Pathophysiology of anti-MAG IgM Gammopathy**

As in other cases of antibody response to carbohydrate structures, anti-MAG IgM antibodies are also thought to arise independent of CD4+ helper T cell help and possibly from B1 cells that do not normally class-switch to T cell-dependent isotypes.<sup>70</sup> Experimental and clinical data suggest that these anti-MAG IgM antibodies in patients are directly pathogenic although the precise mechanism of disease pathogenesis remains unclear. It is believed that the pathological mechanisms could vary depending on the differences in antibody reactivity to the glycoconjugates expressed in different compartments of the nerve. Evidence including the deposits of monoclonal anti-MAG IgM and complement found on the myelin sheaths and therapeutic reduction of antibody titres corresponding to clinical improvement of some patients suggest that these autoantibodies are demyelinating.<sup>75</sup>

The mechanism by which these large IgM molecules can cross the BNB to enter the endoneurium is not well understood. The presumed cascade of pathological

process is possibly caused by a breach and an increased permeability across the BNB followed by the leakage of immunoglobulins into the endoneurial space and a subsequent attack of peripheral myelin and axon.<sup>76,77</sup>

## **2.19 Detection of anti-MAG IgM antibodies**

To detect the presence of anti-MAG antibodies in patients with this gammopathy, the current test in use is a standardized commercial anti-MAG antibody enzyme linked immunosorbent assay (ELISA) from Bühlmann Laboratories, Switzerland, where MAG purified from human myelin or a synthetic HNK-1 is used as antigen. This method of detection has been considered as the gold standard in the detection of anti-MAG IgM antibodies.

Another preferred method of detection includes immunofluorescence analysis of anti-MAG antibodies on nerve biopsy. Patients with sera positive for anti-MAG IgM antibodies stain the myelin sheath of individual axons contained within nerve fibre bundles giving it a unique pattern. This pattern has been used to describe the “typical MAG” reactivity.<sup>78</sup>

Anti-MAG IgM antibodies can also be detected by Western Blotting techniques but ELISA proved more sensitive and allowed more precise quantification of antibody titres when the two methods were compared.<sup>79</sup>

However, none of these methods used as diagnostic tools for the detection of anti-MAG IgM antibodies use recombinant cell based assays expressing HNK-1 glycosylated human MAG.

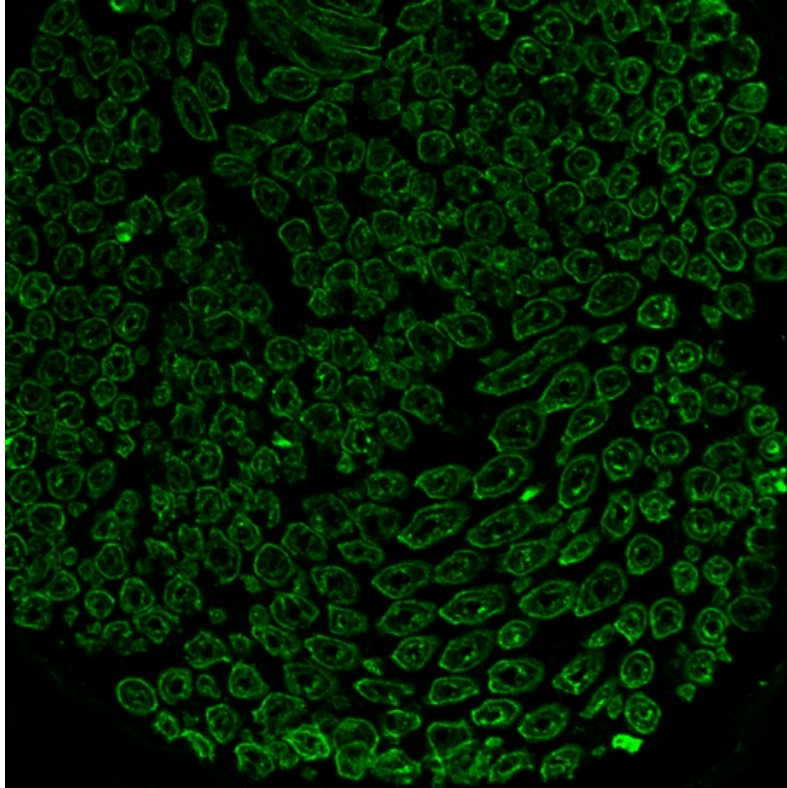


**Figure 6: „Typical MAG“ reactivity seen on peripheral nerve. MAG reactivity can be identified by a classic pattern of widened myelin lamellae. Here is a representative image of anti-MAG IgM antibodies binding to their target antigen when serum from a patient with anti-MAG IgM Gammopathy is incubated on cross section of peripheral nerve from primate (*Makaka mulatta*). IgM was detected using goat anti human IgM fluorescein labelled (Image taken on Zeiss LSM 700, magnification 20x)**

### **3. Aims and objectives**

The overall aim of the thesis was to study the role and detection of antibodies to neuronal antigens in neuroinflammation.

In the event of an ischemic stroke the presence of autoantibodies as a diagnostic biomarker is debatable. In this context, the first objective was to address the possible involvement of stroke induced autoantibodies to neuronal antigens in the outcome of the disease.

On the other hand in a disease like anti-MAG IgM Gammopathy, the antigenic target is well defined. Tissue based IIFT employing sections of peripheral nerve beside ELISA systems based on purified human MAG are in use to detect anti-MAG IgM. However, there is a need to set up assays based on recombinant HNK-1 modified MAG to replace tissue based methods and to increase sensitivity of antibody detection. The second aim of the thesis was to develop sensitive diagnostic tools based on recombinant HNK-1 glycoepitope for the detection of autoantibodies in patients with this peripheral neuropathy.

## 4. Materials and Methods

### 4.1 Buffers, Media and Solutions

Name	Composition
HEK cell culture medium	DMEM (high glucose) supplemented with 10 % FBS
Luria/Miller broth (LB) medium	2.5 % (w/v) LB powder (Carl Roth, Germany) in water
EU-Lysis buffer	100 mM Tris (pH 7.4), 150 mM NaCl, 2.5 mM EDTA, 1 % (v/v) Triton-X-100 and 0.5 % (w/v) deoxycholate made up with water
EU-HEK cell lysis buffer	20 mM Tris-HCl (pH 7.4), 50 mM KCl, 2 mM MgCl <sub>2</sub> and 1 mM Phenylmethylsulfonyl fluoride (PMSF) made up with water
Fixation solution	50 % (v/v) methanol and 10 % (v/v) Acetic acid made up with water
Blue Silver staining solution	5 % (w/v) aluminiumsulfate-(14-18) hydrate, 10 % (v/v) ethanol, 0.02 % (w/v) Coomassie Brilliant Blue, 2 % (v/v) ortho-phosphoric acid in water
Blue Silver destaining solution	10 % (v/v) ethanol and 2 % (v/v) ortho-phosphoric acid in water
TNI-150	5 mM Tris-HCl (pH 8.0), 300 mM NaCl, 150 mM imidazole in water
TNI20M (10x)	55 mM Tris-HCl (pH 8.0), 1.8 M NaCl, 220 mM imidazole, 550 mM magnesium chloride in water
TNI-20	5 mM Tris-HCl (pH 8.0), 300 mM NaCl, 20 mM imidazole in water
TN150E-IEX	20 mM Tris-HCl (pH 8.5), 150 mM NaCl, 2.5 mM EDTA, 1 mM PMSF in water
Biocinchoninic acid-bovine serum albumin (BCA-BSA) standard (stock)	5 mg/mL BCA-BSA (Sigma-Aldrich Chemie, Germany) in 0.9 % (w/v) NaCl in water
BCA-copper sulfate solution	4 % (w/v) copper sulfate in water
TN1000E-IEX	20 mM Tris-HCl (pH 8.5), 1000 mM NaCl, 2.5 mM EDTA, 1 mM PMSF in water
PBS- 0.2 % Tween (PBS-T)	0.2 % Tween <sup>®</sup> 20 in PBS

Ponceau S staining solution	0.2 % (w/v) Ponceau S and 7 % (v/v) acetic acid in water
-----------------------------	--

## 4.2 Antibodies

Name	Isotype/ clonality	Use	Dilution	Company
Anti-HNK-1 antibody	IgM; mouse monoclonal	Indirect immunofluorescence test (IIFT); immunoblot, neutralization assay, ELISA	Assay dependent	Sigma-Aldrich Chemie, Germany/ EUROIMMUN, Germany
Anti-MAG antibody	IgG; rabbit polyclonal	Immunoblot	1:1000	Sigma-Aldrich Chemie, Germany
Goat anti-mouse IgM	IgM	IIFT; immunoblot	Assay dependent	Sigma-Aldrich Chemie, Germany
Goat anti-rabbit IgG	IgG	Immunoblot	1:2000	Sigma-Aldrich Chemie, Germany
Anti-His antibody	IgG; monoclonal	Immunoblot	1:1000	EUROIMMUN, Germany
Goat anti-human IgG/ IgM/ IgA antibody	IgG, IgM, IgA	IIFT; ELISA	Ready-to-use	EUROIMMUN, Germany

## 4.3 Human sera

68 ischemic stroke patients and 21 age-matched control subjects free from acute neurological diseases from the “Immunological Biomarkers in Patients With Acute Ischemic Stroke” study (Clinicaltrials.gov identifier NCT01894529) for which all serum samples (days 0, 1, and 90) were available were included in the study. The patients or legal representatives as well as control donors provided informed consent for this study. The serum samples were stored at the



Functional Unit of Cerebrovascular Diseases Biologic Sample Collection, which is registered in the Hospital Clínic – IDIBAPS Biobank.

Anonymized serum samples of patients with anti-MAG IgM Gammopathy were provided by the Glasgow Neuroimmunology Biobank (Integrated research application system (IRAS) project number 83681). Two cohorts with sizes of 13 and 32 samples respectively, were used in the study for the development of two different diagnostic tools to detect antibodies in patients with anti-MAG IgM gammopathy. The first cohort of serum samples with very high ELISA-titer (pre-tested using anti-MAG ELISA from Bühlmann Laboratories, Switzerland) were used for the initial test setup of the first assay. The latter cohort of 32 serum samples (just pre-characterized as “positive”, but not necessarily with a high titer) were used for the final validation of both the assays.

Serum samples from healthy blood donors used as controls for the study were received from the EUROIMMUN internal serum collection.

#### **4.4 Indirect immunofluorescence test (IIFT)**

The EUROIMMUN BIOCHIP Mosaics™ use several glass slides coated with different combinations of substrates side by side on the same reaction field such that antibodies binding to various tissue sections, cells and/or antigen dots can be investigated simultaneously.<sup>80</sup> The respective substrates are treated in different ways and the BIOCHIP Mosaics™ are produced so as to fit the need of the particular study under investigation.

For the IIFT, the standard EUROIMMUN protocol was followed.

Briefly, sera from patients or healthy blood donors were diluted at 1:10 or 1:100 in PBS-0.2 % (v/v) Tween (PBS-T). Antibodies used as positive controls were diluted according to the manufacturer’s guidelines. Diluted serum samples were pipetted out on each of the reagent support tray and then carefully covered with the BIOCHIP Mosaic™ ensuring that the substrate was in contact with the samples. The volume of serum or primary antibody dilution varied between 30 µL and 65 µL depending on the format and design of the respective BIOCHIP

Mosaic™ used. The IIFT substrates were then incubated at room temperature (RT) for 30 minutes.

This was followed by a washing step with PBS-T and incubation in a PBS-T filled cuvette for 5 minutes. For the human sera, 30 µL to 60 µL of Fluorescein isothiocyanate (FITC)-conjugated goat anti-human IgG, IgM or IgA secondary antibody (EUROIMMUN, Germany) was pipetted out on separate reagent supports and the Mosaics were incubated for 30 minutes at RT, protected from direct sunlight. For commercially available primary antibodies, their appropriate fluorochrome conjugated secondary antibodies were used in the same manner as described above.

A list of the primary and secondary antibodies used for the different studies have been added in Chapter 4.2.

The washing step was repeated with PBS-T and incubation in the same buffer for five minutes. The BIOCHIP Mosaics™ were then processed for microscopy by pipetting about 10 µL of embedding medium (EUROIMMUN, Germany) onto glass coverslips which were then inverted over the BIOCHIPS.

Examination of specific antigen-antibody pattern was done using a Zeiss *Axioskop 2* and images were taken using a LuCam Camera (Lumenera Corporation, Canada) and the supplied Software LuCam Capture 5.0. For some experiments, the confocal microscope LSM 700 (Zeiss, Germany) and the appropriate software ZEN 2009 were used. Reading of immunofluorescence patterns and microscopy were performed between 24-48 hours after incubation.

## 4.5 DNA *in vitro* cloning and recombinant protein expression

### 4.5.1 Expression plasmids used

All expression plasmids used were derived from pTriEx-1 (Merck Biosciences, Germany).

Table 2: List of expression plasmids and the corresponding proteins expressed.

Expression plasmids	Expressed protein
pTriEx-1-MAG (dHis)	MAG without His-tag
pTriEx-1-pre-MAG(ec)-H <sub>6</sub>	Secreted MAG with His-tag
pTriEx-1-HNK-1ST (dHis)	HNK-1ST without His-tag
pTriEx-1-GlcAT-P (dHis)	GlcAT-P without His-tag
pTriEx-1-GlcAT-P [E284A] (dHis)	Mutant GlcAT-P without His-tag

The cDNAs that were used for cloning of the different proteins, including those with modifications, have been listed in Table 3.

Table 3: List of cDNAs used for the expression of the different proteins.

cDNA	GenBank accession number	UniProt accession number
HNK-1 sulfotransferase (HNK-1ST)	BC010441	O43529
Galactosylgalactosylxylosylprotein 3-beta-glucuronosyltransferase 1 (GlcAT-P)	BC010466	Q9P2W7
Myelin associated glycoprotein (MAG)	BC053347	P20916

### 4.5.2 Construction of Expression Plasmids

Vector NTI Advance 11.5.4 (Invitrogen, Germany) was used for planning of all cloning procedures as well as for the construction of DNA-sequences, including generation of primers and restriction analyses.

**Table 4: The primers and their respective sequences that were used for the construction of the different expression constructs.**

<b>List of primers</b>	<b>Sequence</b>	<b>Restriction Enzyme</b>
sense MAG	ATAGGTCTCACATGATATTCCTCACGGCAC TGCCTCTG	Eco31I
asense MAG-Stop	ATAGGTCTCTTCGAGTCACTTGACCCGGAT TTCAGCATACTC	Eco31I
asense MAG (ec)	ATAGGTCTCTTCGAGAGGCCCGATCTTGCC CCACATCAGTC	Eco31I
sense HNK- 1ST	ATAGAAGACATCATGCACCACCAGTGGCTT CTGCTGGC	BbsI
asense HNK- 1ST-Stop	ATAGAAGACCGTCGAGTTAGTTTAGCAAAA AGTCTGGTTTC	BbsI
sense GlcAT- P	ATAGGTCTCACATGCCGAAGAGACGGGACA TCCTAGC	Eco31I
asense GlcAT-P	ATAGGTCTCATCGAGTCAGATCTCCACCGA GGGGTCAGTG	Eco31I
asense GlcAT-P- E284A-ZF1	ATAGGTCTCATAGCCTGGTAGCCTCCCTTC ACACCTCGCAG	Eco31I
sense GlcAT- P-E284A- ZF2	ATAGGTCTCAGCTAGCAGCCTCCTTCGAGA ACTTGTCAC	Eco31I

#### 4.5.3 Amplification of DNA Fragments by PCR

Enzymes and buffers of the High Fidelity PCR Enzyme Mix (Fermentas Molecular Biology, Germany) were used for cloning and amplification of the DNA target sequence of interest. Taq DNA Polymerase LC (Fermentas Molecular Biology, Germany) was used for analytical PCR. Compositions of the reaction mixes were as follows:

***High Fidelity (HF) reaction mix***

1 x High Fidelity PCR Buffer  
0.2 mM dNTPs each  
1  $\mu$ M primers each  
1 ng template DNA  
0.1 U/ $\mu$ L High Fidelity PCR Enzyme Mix

***Taq DNA Polymerase LC reaction mix (equivalent to HF set up)***

1 x PCR Buffer  
2 mM MgCl<sub>2</sub>  
0.2 mM dNTPs each  
1  $\mu$ M primers each  
10 ng template DNA or 2  $\mu$ L bacterial culture  
1.25 U Taq Polymerase LC

***PCR procedure***

melting: 30 s at 94 °C  
annealing: 45 s at 56 °C  
amplification: 1 min per kb at 72 °C  
repetition: 30 times

PCR cleanup was done with NucleoSpin® Extract II (Macherey-Nagel, Germany) according to the manufacturer's instructions.

**4.5.4 Digestion by Endonucleases**

All restriction enzymes, conventional as well as FastDigest® enzymes and their appropriate buffers, were purchased from ThermoFisher Scientific, Germany. Depending on the different combination of restriction enzymes used, the composition of the restriction mix varied appropriately and this was followed according to the manufacturer's guidelines.

Purification of digested DNA fragments was either done with NucleoSpin® Extract II (Macherey-Nagel, Germany) or by agarose gel preparation using the same kit.

#### **4.5.5 Ligation and Transformation**

Rapid DNA Ligation Kit (ThermoFisher Scientific, Germany) was used for ligation of DNA fragments. The reaction was done at room temperature (RT) for 10 minutes in a total volume of 20 µL consisting of 100 ng vector DNA, 200 – 500 ng insert DNA, 1 x Rapid Ligation Buffer and 5 Units T4 DNA ligase.

Following ligation, the reaction mix was used for transformation into competent NEB® 5-alpha *E. coli* (New England BioLabs GmbH, Germany). After adding the DNA to the cell suspension it was incubated for 10 minutes at 0°C. The heat shock was done at 42 °C for 45 seconds, followed by a one-minute-incubation at 0°C. Four volumes of LB medium were added and incubated at 37 °C for 30 minutes on shaking. Most of the supernatant was removed after a centrifugation step at 21,000 g for 2-3 minutes at 4 °C (about 100 µL of medium left). The cells were then resuspended in the remaining supernatant and plated onto LB agar plates supplemented with ampicillin (100 µg/mL) for selection. Plates were incubated at 37 °C over night.

#### **4.5.6 Plasmid Preparation and Sequencing**

Clones were inoculated in 5 mL LB medium with 100 µg/mL ampicillin and incubated over night at 37 °C under shaking. The following day plasmids were purified using NucleoSpin® Plasmid (Macherey-Nagel, Germany) and the inserted DNA sequenced at SeqLab Sequence Laboratories, Germany. Evaluation of DNA sequences was done using ContigExpress 11 and Vector NTI Advance 11.5.4 (Invitrogen, Germany).

#### **4.5.7 Generation of recombinant IIFT substrates**

HEK293 cells were seeded onto glass slides (EUROIMMUN, Germany) using DMEM high glucose medium supplemented with 10 % (v/v) FBS and antibiotics Penicillin (100 U/mL) and Streptomycin (0.1 mg/mL). Following incubation at 37 °C, 95 % rH and 8.5 % (v/v) CO<sub>2</sub> for four hours, the cells were transfected with the appropriate plasmid(s) using ExGen 500 (Biomol GmbH, Germany) according to the manufacturer's instructions. Non modified pTriEx-1 was used as negative control. The transfected HEK293 cells were incubated at 37 °C, 95 % relative humidity and 8.5 % CO<sub>2</sub> for 48 hours. The cells were formalin fixed and dried on glass slides and were subsequently used for BIOCHIP production.<sup>81</sup>

#### **4.6 Immunoprecipitation analysis**

HEK-cells were obtained by flushing out  $2 \cdot 10^8$  cells from 1 HYPERFlask<sup>®</sup> cell culture vessel (Corning, United States), washed with 6 mL ice cold PBS (EUROIMMUN, Germany) and centrifuged at 21,000 g for 10 minutes to get the washed cell fraction.

This sediment was gently solubilized by adding 9 volumes of EU-Lysis buffer to 1 volume of cells and sonicated three times for 10 seconds each with a pause of 5 seconds in between on ice.

Lysate mix preparations containing 500 µL HEK cell lysate (further diluted or undiluted), 5 µL Phenylmethylsulfonyl fluoride (PMSF) (Sigma-Aldrich Chemie, Germany) and 30 µL diluted (1:10 or 1:100) primary antibody, were gently mixed and incubated for three hours at 4 °C on a rotator.

Afterwards, the lysate mixes were centrifuged at 16,000 g for 10 minutes at 4 °C. The supernatant was collected and 15 µL of Bio-Adembeads antibodies goat anti-mouse IgM (Ademtech, France) was added.

For experiments using Dynabeads<sup>®</sup> Protein G (ThermoFisher Scientific, Germany), the beads were first equilibrated following manufacturer's guidelines and then 50 µL of the beads were added to the lysate mix preparation.

The next step was an over night incubation at 4 °C on a rotator. The following day, the tubes containing the lysate mix were placed on a DynaMag<sup>™</sup>-2 Magnet

(ThermoFisher Scientific, Germany) for 2-5 minutes and the supernatant was removed. Positively selected antigen-antibody complexes attached to the Beads were then washed five times with 500  $\mu$ L of EU-Lysis buffer. Following the final washing step, the tubes were changed, the supernatant was discarded and the tubes were removed from the magnetic field.

A “master mix” of NuPAGE<sup>®</sup> LDS Sample Buffer was prepared using the following recipe:

1 x NuPAGE<sup>®</sup> LDS (ThermoFisher Scientific, Germany)

25 mM 1,4-Dithiothreitol (DTT) (Gerbu Biotechnik GmbH, Germany)

diluted in water

40  $\mu$ L of the master mix were added into each of the tubes and incubated at 70 °C for 10 minutes on a shaker. The tubes were placed back on the magnetic field. The supernatant was collected into a fresh tube and the beads were discarded. 4  $\mu$ L iodoacetamide solution (20% (w/v)) was added to each of the tubes followed by an incubation at RT in the dark for 30 minutes.

These samples were used for subsequent sodium dodecyl sulfate polyacrylamide gel electrophoresis (SDS-PAGE) and/or Western Blotting.



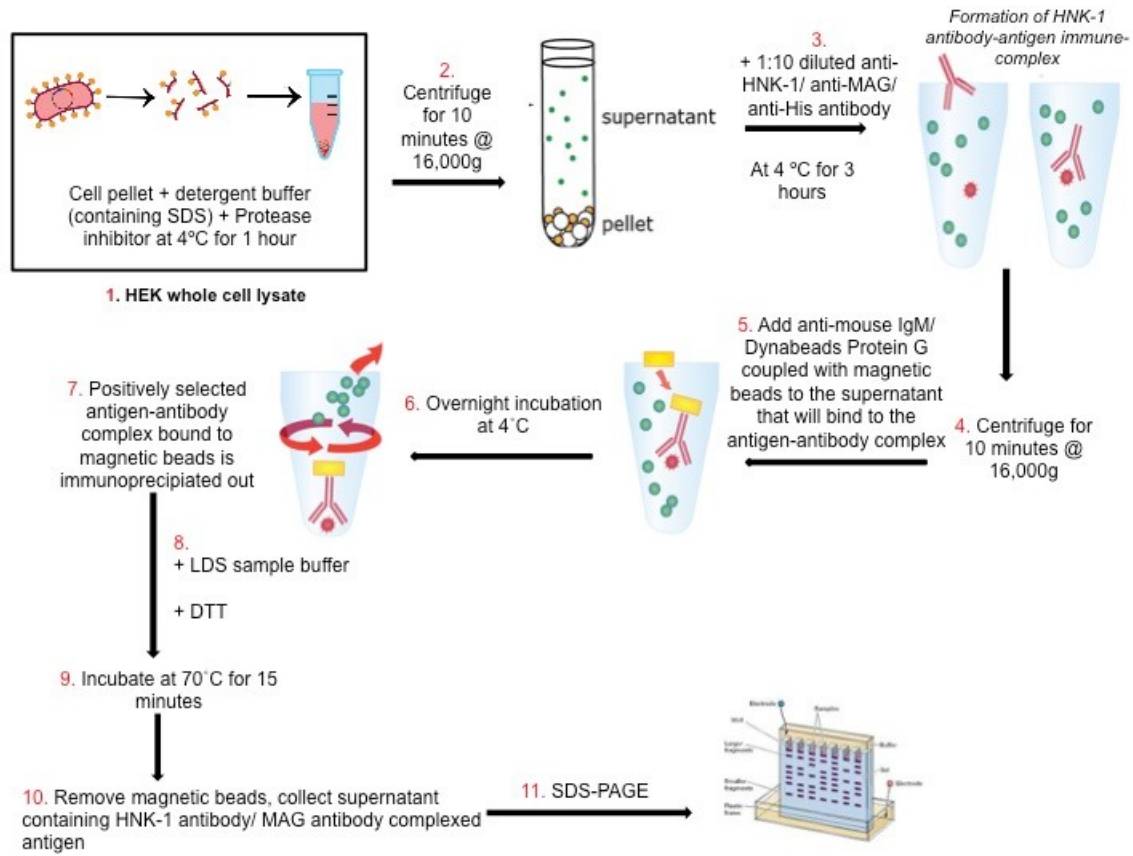


**Figure 7: A schematic representation of the immunoprecipitation protocol.**

NuPAGE® 4-12 % Bis-Tris gels (Invitrogen, Germany) were used for SDS-PAGE according to the manufacturer's instructions using the appropriate MOPS electrophoresis buffer. The proteins were blotted onto a nitrocellulose membrane (Sartorius AG, Germany) in 60 minutes at 400 mA using NuPAGE® Transfer Buffer. Successful transfer of the proteins onto the membrane was confirmed by a 10 minute incubation of the nitrocellulose membrane in Ponceau S staining solution. Destaining was done using 50 mM Tris-base (Gerbu Biotechnik GmbH, Germany). The membrane was blocked with WaPu Plus (EUROIMMUN, Germany) for 45 minutes under shaking. Primary and their corresponding secondary antibodies were diluted in the same blocking buffer and incubated overnight or for one hour respectively. Between the incubation steps, the membrane was washed using Western Blot washing buffer (EUROIMMUN, Germany) three times for five minutes each under shaking. Protein bands were

visualized with Nitro blue tetrazolium (NBT)/5-bromo-4-chloro-3-indolyl-phosphate (BCIP) (EUROIMMUN, Germany). The staining reaction was stopped with distilled water.

For Blue Silver staining, the gel was incubated with Fixation solution for 30 minutes at RT under slight shaking. After discarding the Fixation solution, staining was done with Blue Silver staining solution overnight at RT for proper visualization of the protein bands. For destaining, Blue Silver destaining solution was used for 30 minutes.

#### **4.7 Transfection of HEK293 cells for protein purification**

HEK293 cells were transfected with plasmid DNA pTriEx-1-pre-MAG(ec)-H6; pTriEx-1-GlcAT-P(dHis) or pTriEx-1-HNK-1ST(dHis) following the standard EUROIMMUN protocol. Briefly, cells were seeded into HYPERFlask® cell culture vessels (Corning, United States) with a density of  $2.3 \cdot 10^5$  cells/mL using HEK cell culture medium. The cells were allowed to settle down for four hours at 37 °C, 95 % relative humidity (RH) and 8.5 % (v/v) CO<sub>2</sub>. Afterwards, they were transfected using ExGene 500 according to the manufacturer's instructions. Protein expression was done for five days as described before. The cell culture supernatant was harvested and cell debris was removed by centrifuging for five minutes at 3400 g.<sup>82</sup>

#### **4.8 Immobilized metal affinity chromatography (IMAC)**

His-tagged proteins were purified by IMAC using an ÄKTA™ pure chromatography system (GE Healthcare GmbH, Germany).

First, the sample load was prepared by adding 1/10 volume of TNI20M (10x) of cell culture supernatant. The pH was adjusted to 8.0 and 0.09 % (v/v) of Triton X-100 was added to the mixture which was then slowly stirred for 30 minutes at RT. Following a centrifugation step at 17,700 g at RT for 30 minutes, the supernatant was filtered with Whatman® cellulose acetate of 0.8 µm pore size (Sigma-Aldrich

Chemie, Germany). The non solubilized material was discarded. An aliquot of the filtrated sample was set aside for analysis.

Nickel Rapid Run™ (Agarose Bead Technologies, Spain) was transferred into a HiScale column (GE Healthcare GmbH, Germany).

For running the IMAC, the default flow rate was set as 10 mL/min. The matrix was washed with four column volume (CV) of filtered distilled water and equilibrated with one CV TNI-150 and six CV TNI-20. One Liter of sample was loaded per 10 mL bed volume at 5 mL/min. The matrix was washed with six CV TNI-20 and isocratic elution of the protein was done with four CV TNI-150 at 5 mL/min. Fractions of 1/5 of the bed volume were collected and subsequently analyzed by Western Blot to check for the presence of the His-tagged protein.

The relevant fractions were pooled and concentrated. The buffer was exchanged against TN150E-IEX five times using 10 kDa ultrafiltration units (Vivaspin, Sartorius, Germany). A bicinchoninic acid assay (BCA) was performed (Chapter 4.11) to determine the concentration of the protein before aliquoting the protein sample and freezing them until the further purification process (Ion exchange chromatography).

#### **4.9 Ion exchange chromatography (IEX)**

Q Sepharose™ Fast Flow (GE Healthcare Life Sciences, Germany) packed in a Tricorn 10/20 column (GE Healthcare Life Sciences, Germany) was used for the purification of HNK-1 glycosylated MAG. IEX was run using the ÄKTA™ pure chromatography system (GE Healthcare GmbH, Germany), following the manufacturer's guidelines.

The flow rate was set to 2 mL/min. The matrix was first regenerated with 10 CV of TN-1000E-IEX and washed with 5 CV of TN1000E-IEX. A sample load of 1 mL was applied at a rate of 0.1 mL/min. A gradient elution of the protein was done from 0 – 100 % upflow from TN150E-IEX to TN1000E-IEX over 20 CV at 1 mL/min. Fractions were collected corresponding to peaks proportional to 280 nm absorption and subsequently analyzed by Western Blot to check for the presence of the HNK-1 glycosylation.

#### **4.10 Neutralization assay**

For the neutralization of the antibody by its corresponding antigen, a soluble form of the antigen was incubated with the antibody (serially diluted from 1:10 to 1:1,000,000) for 30 minutes at RT on a rotator. Following a centrifugation at 21,000 g the supernatant was tested by IIFT on a BIOCHIP Mosaic™ containing the cell bound antigen. In parallel, the antibody alone (also serially diluted from 1:10 to 1:1,000,000) was tested by IIFT on cell bound antigen.

#### **4.11 Bicinchoninic acid (BCA) assay**

20 µL of Bicinchoninic acid-bovine serum albumin (BCA-BSA) standards were applied into individual wells of a 96-well microtitre plate (Greiner Bio-one, Austria). 20 µL of the test protein solution (undiluted) and dilutions 1:10 and 1:100 were pipetted in duplicates. BCA-copper sulfate solution was prepared at a 50:1 mixture and 200 µL of it was added into each of the wells and incubated for 30 minutes at 37 °C. The reading was done at 560 nm using a Sunrise™ microplate reader (Tecan, Switzerland).

#### **4.12 Enzyme linked immunosorbent assay (ELISA)**

Nunc MaxiSorp® (Sigma-Aldrich Chemie, Germany) ELISA plates were coated with 100 µL/well of purified protein MAG using a concentration of 1 µg/mL in PBS-coating buffer (EUROIMMUN, Germany) for 3 hours at RT. The coating solution was removed and the coated ELISA plates were incubated with Casein blocking buffer (EUROIMMUN, Germany) at a volume of 200 µL/well for 1 hour at RT. The plates were washed thrice with ELISA wash buffer (EUROIMMUN, Germany) using a microplate washer (EUROIMMUN, Germany), followed by incubation with 100 µL/well of serum or plasma samples from patients or healthy blood donors diluted in Casein sample buffer (EUROIMMUN, Germany) for 30 minutes at RT. The ELISA plates were washed thrice followed by a second incubation with 100 µL/well of ready-to-use anti-human IgM-peroxidase (POD)

(EUROIMMUN, Germany) for 30 minutes at room Temperature. After three 200  $\mu\text{L}$ /well washing steps, 100  $\mu\text{L}$ /well of ELISA substrate (EUROIMMUN, Germany) was added to every well and the plates were incubated for 15 minutes, in the dark. To stop the reaction, 100  $\mu\text{L}$ /well Stop solution (EUROIMMUN, Germany) was added and the plates were read at measuring wavelength of 450 nm (reference at 620 nm) using a absorbance microplate reader (Tecan, Switzerland).

## **5. Results**

### **5.1 Stroke does not induce autoantibodies against neuronal structures**

The presence of autoantibodies with specificity for neuronal structures were investigated by IIFT using sections of rat cerebellum and hippocampus, primate cerebellum, intestine, nerve and pancreas. The IIFT substrate also contained acetone fixed NMDAR NR1a subunit and Glutamate decarboxylase-65 (GAD65) transfected cells and formalin fixed Gamma-aminobutyric acid-B receptor (GABA<sub>B</sub>R), Aquaporin-4 (AQP4), Leucine-rich, glioma inactivated 1 (LGI1) and contactin-associated protein-like 2 (CASPR2) transfected HEK293 cells as substrates.

Serum samples from 68 ischemic stroke patients collected at three different time points (day 0, day 1 and day 90 following stroke) and 21 serum samples from age and sex matched healthy controls were analysed at a dilution of 1:10.

A qualitative analysis of autoantibodies already present in serum samples on days 0 and 1 after stroke were considered to reflect previous autoreactivity while patients showing autoreactivity at day 90 but not in the samples taken at the previous time points were considered to have developed new reactivity.

A cut-off system based on the recommended semi-quantitative evaluation values ([www.euroimmun.com](http://www.euroimmun.com)) was followed while analysing the immunofluorescence patterns and their intensity. A scoring system of 1-5 was used to assign a semi-quantitative value to the titre of antibody that is present with 1 indicating very low titres of antibodies present in the sample to a specific antigen at that given dilution and 5 showing very high titres of the antibody to the antigen.

The antibody response has further been subgrouped individually as IgG, IgM and IgA subclasses indicating the use of FITC conjugated anti-human IgG, anti-human IgM or anti-human IgA as secondary antibodies respectively.

#### **5.1.1 The IgG response**

A baseline low reactivity to a panel of “commonly identified autoreactivities” ([www.euroimmun.com](http://www.euroimmun.com)) at 1:10 serum dilution was identified in the sera of almost all stroke patients as well as in the healthy controls. The baseline low level reactivity to these “commonly identified antigens” has been referred to as “diagnostically irrelevant” and have therefore not been scored. There were no further indications of autoantibodies of the IgG isotype to neuronal structures in stroke patients.

### **5.1.2 IgM response**

Similar to the IgG response, majority of the patients analysed had reactivity of IgM with baseline or even lower immunofluorescence intensity to common antigens like neurofilament and myelin components. However, because this low baseline level of IgM antibody response at 1:10 serum dilution was below the qualitative cut-off and a similar frequency was detected in healthy controls as well, these fluorescent intensities have also not been accounted for.

One patient harboured antibodies to neurofilament detected on rat as well as primate CNS tissue sections. The reactivity had an unchanged intensity of 3 on all three time points of serum collection.

Seven patients (10.2 %) of the stroke cohort had antibodies to the NR1 subunit of NMDAR detected only on the transfected HEK293 cells on all three days of serum collection. Although the standard verification method of antibodies binding to NMDAR is seen on rat brain tissue as an intense reactivity involving the hippocampus, in this case no such detection was observed on tissue sections.

### **5.1.3 IgA response**

Six patients (8.8 %) had antibodies to the NR1 subunit of NMDAR transfected HEK293 cells on all three days of serum collection with one patient’s serum showing a high intensity of 4. Similar to the IgM response, no detection was observed on brain tissue sections. Interestingly, one healthy control had antibodies to NMDAR subunit NR1 of intensity 2 at serum dilution 1:10 as detected on the transfected HEK293 cells.

In summary, no autoantibody profile for serologic detection of stroke induced autoimmunity were found.

## 5.2 Cloning of MAG/ MAG(ec), GlcAT-P, HNK-1ST and GlcAT-P [E284A]

The antigenic target in patients with anti-MAG IgM Gammopathy is the HNK-1 glycoepitope. The first objective of this study was to generate this HNK-1 glycoepitope in the HEK293 cell based system. The two key enzymes involved in the synthesis of the HNK-1 glycoepitope are Glucuronyltransferase (GlcAT-P) and HNK-1 Sulfotransferase (HNK-1ST).

**Table 5: Summary of the cloning strategy for GlcAT-P and HNK-1ST.**

<b>Name of enzyme</b>	<b>Template sequence</b>	<b>Sense Primer</b>	<b>Antisense Primer</b>	<b>Restriction</b>
GlcAT-P	IMAGE ID 4157589  Sequence Clone Accession BC010466	ATAGGTC TCACATG CCGAAGA GACGGG ACATCCT AGC	ATAGGTC TCATCGA GTCAGAT CTCCACC GAGGGG TCAGTG	Eco31I
HNK-1ST	IMAGE ID 4158309  Sequence Clone Accession BC010441	ATAGAAG ACATCAT GCACCAC CAGTGGC TTCTGCT GGC	ATAGAAG ACCGTCG AGTTAGT TTAGCAA AAAGTCT GGTTTC	BbsI



Briefly, sense and antisense primers were used for the amplification of the cDNA employing the full length cDNA clones listed in Table 3. Eco31I or BbsI restriction enzymes were used to generate an overhang in the amplified sequence to allow integration into NcoI/XhoI linearized pTriEx-1 vector. In pTriEx-1 transcription is controlled by the Chicken Beta actin promoter fused to the immediate early cytomegalovirus (CMV) transcriptional enhancer. To get rid off potential artificial splicing within the cDNA encoded transcript, an intron flanked by exons is encoded 5' non translated region (5' NTR) of the transcript allowing controlled splicing within the 5' NTR.

The ligation reaction was directly used to transform *E. coli* and subsequently spread on LB-agar plates with 100 µg/mL ampicillin (Ap) and incubated over night at 37°C. Next day 10 individual clones were used to inoculate 5 mL LB medium supplemented with 100 µg/mL ampicillin to be used for plasmid purification.

To analyze for recombinant plasmids the purified DNA was cut using XbaI/XhoI and separated on a 0.8% (w/v) Agarose gel using TAE running buffer. The DNA was visualized under blue light employing CyberSafe fluorescence.

As in the case of most glycotransferases, GlcAT-P is also a type II membrane protein comprising a short N-terminal cytoplasmic tail, a transmembrane domain and a large C-terminal catalytic domain.<sup>83</sup> This transmembrane nature of GlcAT-P makes it plausible that the antigenic epitope recognized by the anti-MAG IgM antibodies might be located on the enzyme itself. Therefore, a mutant variant (E284A) of the GlcAT-P enzyme was also prepared with a point mutation located at an active site of the enzyme. This mutation would only minimal interfere with the structure of the enzyme but only inhibit the enzymatic activity of GlcAT-P.<sup>62,</sup>

84

The point mutation on wildtype GlcAT-P amino acid sequence is at the 284th position, where a glutamic acid residue (E) is replaced by alanine (A).

**Table 6: Comparison of amino acid sequences between the wildtype and inactive GlcAT-P.**

<b>Name of protein</b>	<b>(Partial) amino acid sequence</b>
Wildtype GlcAT-P	... VKGGYQ <b>E</b> SSSLRELVTL ...
GlcAT-P (E284A)	... VKGGYQ <b>A</b> SSSLRELVTL ...

For the cloning strategy, briefly, two sets of primers (sense primer GlcAT-P and asense primer GlcAT-P-E284A-ZF1; sense primer GlcAT-P-E284A-ZF2 and antisense GlcAT-P-Stop) were used to amplify the template cDNA of wildtype GlcAT-P to generate two different fragments: GlcAT-P[E284A]-ZF1 and GlcAT-P[E284A]-ZF2. Both fragments were digested using Eco31I restriction enzymes. Both fragments were then ligated into the pTriEx-1 vector to give pTriEx-1-GlcAT-P[284A].

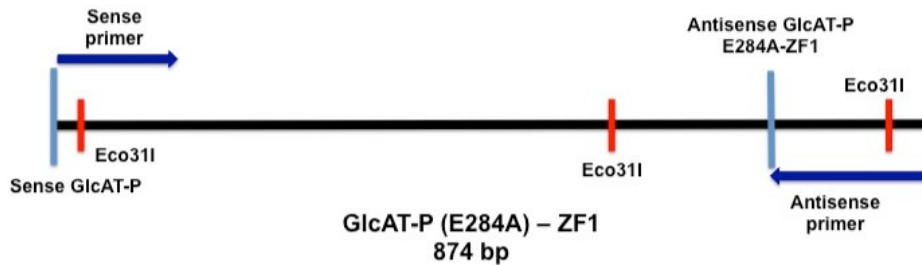


**Figure 8A: Cartoon of fragment (ZF1) of GlcAT-P(E284A).**



**Figure 8B: Cartoon of fragment (ZF2) of GlcAT-P(E284A).**

Expression construct for full length human MAG or the **extracellular (ec)** domain of MAG fused with a C terminal His-tag were also generated and the DNA sequence verified. Cloning was based on the strategies described above.

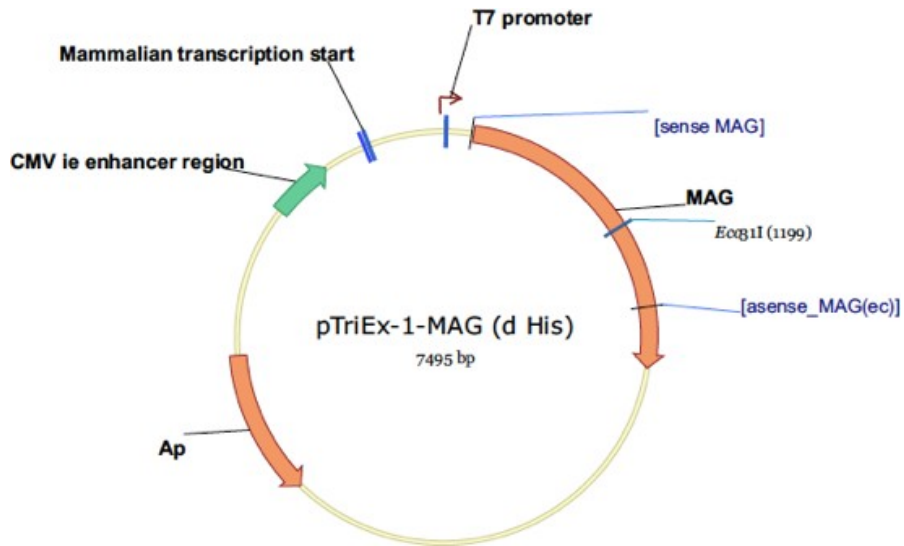


Figure 9: Overview of the expression construct for full length human MAG.

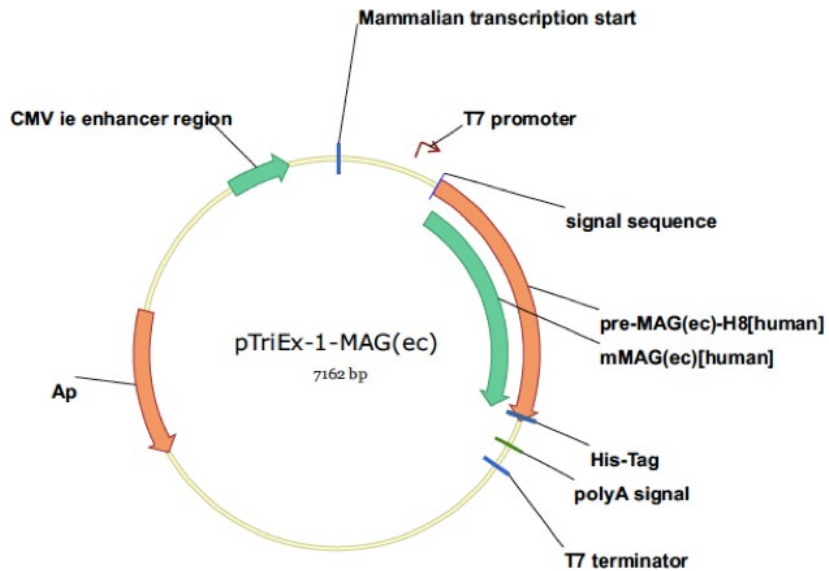


Figure 10: Overview of the expression construct for MAG(ec).

### 5.3 Generation of HNK-1 target antigen by recombinant techniques

HEK293 cells were transfected or co-transfected with either one or both the DNA encoding enzymes and with or without MAG. Formalin fixed non permeabilized transfected cells were subsequently used for the generation of BIOCHIP Mosaics™. Successful expression of HNK-1 glycoepitope by transfection of the enzymes was tested using a commercial mouse anti-HNK-1 IgM antibody (Sigma-Aldrich Chemie, Germany) as positive control.

Table 7: HNK-1 antigen BIOCHIP Mosaic. This table summarizes the scheme of the BIOCHIPs with transfected HEK293 cells and their corresponding reactivity using a commercial anti-HNK-1 antibody.

Transfection scheme	HNK-1 glycosylation
MAG	No
MAG+GlcAT-P	<b>Yes</b>
MAG+HNK-1ST	No
MAG+GlcAT-P+HNK-1ST	<b>Yes</b>
GlcAT-P	<b>Yes</b>
HNK-1ST	No
GlcAT-P+HNK-1ST	<b>Yes</b>

As shown in Figure 11, all GlcAT-P transfected HEK293 cells were immunoreactive when incubated with the mouse anti-HNK-1 IgM antibody. This reactivity was independent of transfection with protein MAG or with the enzyme HNK-1ST. However, this was not the case with either only HNK-1ST- or MAG-transfected HEK293 cells. This was a clear indication that in this system the limiting enzyme for the formation of the HNK-1 glycoepitope is GlcAT-P.

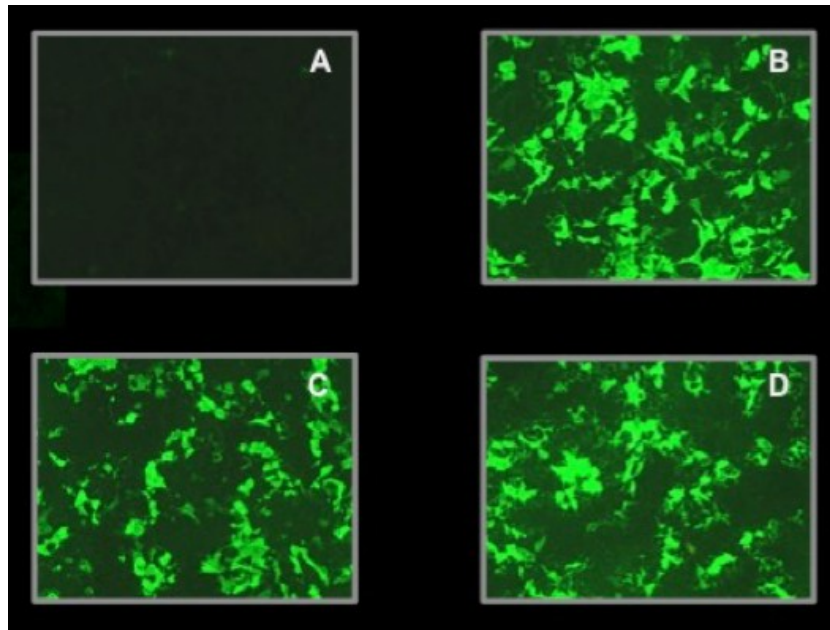
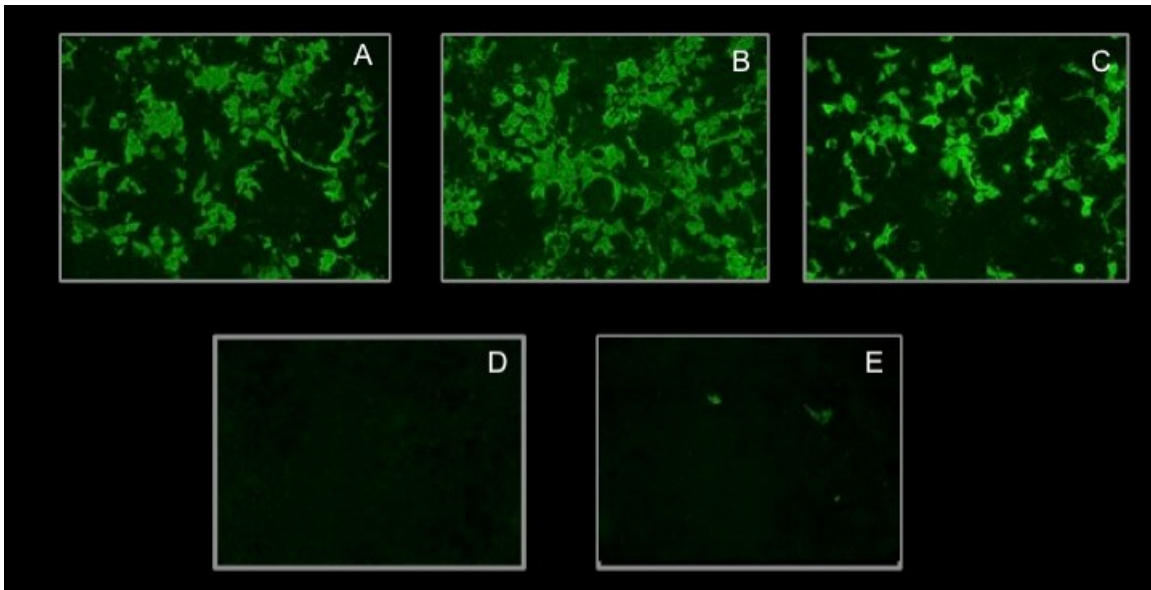


Figure 11: GlcAT-P alone has to be supplemented to generate MAG-independent HNK-1-glycoepitope in HEK293 cells. HEK293 cells transfected with plasmids encoding (A) MAG (B) GlcAT-P, (C) MAG+GlcAT-P and (D) MAG+GlcAT-P+HNK-1ST were formaline fixed and incubated with mouse anti-HNK-1-IgM. Bound IgM was detected using anti-mouse-IgM-FITC. When GlcAT-P is expressed in HEK293 cells, the HNK-1 glycoepitope can be detected. This indicates that only GlcAT-P is required in HEK293 cells to generate the HNK-1-glycoepitope whereas, HNK-1ST is already present in this cell system.

## 5.4 Antibody binding to HNK-1 target antigen in HEK293 cells is GlcAT-P dependent

Successful expression of the HNK-1 glycoepitope on the HEK293 cells was verified using the mouse anti-HNK-1 IgM monoclonal antibody. The next objective was to confirm HNK-1 immunoreactivity on these transfected cells using sera from patients with anti-MAG IgM Gammopathy. Serum samples of 13 patients with anti-MAG IgM Gammopathy and control sera (5 healthy blood donors and 8 patients with Relapsing-remitting multiple sclerosis) were incubated on the transfected cells on BIOCHIP Mosaics™ at dilutions 1:10 and 1:100 followed an incubation with anti-human-IgM-FITC.



**Figure 12: Confirmation of the antigenic target of „anti-MAG antibodies“ in patients with anti-MAG/HNK-1 IgM Gammopathy. All GlcAT-P transfected HEK293 cells, in the presence or absence of MAG and/or HNK-1ST, show a positive reactivity with sera from patients with anti-MAG IgM Gammopathy. In the absence of the enzyme GlcAT-P, there is no binding of anti-MAG/HNK-1-IgM. This re-confirms the presence of GlcAT-P as being essential in the formation of the HNK-1 glycoepitope in the HEK293 cells. The images represent (A) MAG+GlcAT-P (B) GlcAT-P (C) MAG+GlcAT-P+HNK-1ST (D) MAG alone (E) MAG+HNK-1ST transfected HEK293 cells, incubated with serum from a patient with anti-MAG IgM Gammopathy at dilution 1:10. Bound IgM was detected using anti-human-IgM-FITC.**

All sera from patients with the peripheral neuropathy showed antibody binding to HEK293 cells expressing the enzyme GlcAT-P, independent of co-transfection with either MAG or the enzyme HNK-1ST. Whereas, in HEK293 cells co-transfected with both MAG and GlcAT-P or MAG and both the enzymes, it is possible that MAG was being HNK-1 glycosylated. This reactivity was also specific only for patients with anti-MAG IgM Gammopathy that harboured anti-HNK-1 IgM antibodies. This result confirmed that HNK-1 glycosylation in HEK293 cells was dependent on GlcAT-P expression in this cell system.

## **5.5 Generation of GlcAT-P [E284A] mutant transfected HEK293 cells**

To investigate whether that the transmembrane GlcAT-P itself is an antigenic target in these patients with anti-MAG IgM Gammopathy, the inactive enzyme

with a point mutation (E284A) was cloned. This mutated protein was expressed on HEK293 cells and the cells were formalin fixed as in the case of the wild-type GlcAT-P. Serum samples were diluted at 1:10 and incubated on both the mutant as well as the wild-type GlcAT-P transfected HEK293 cells. For every sample incubated on the two substrates, the fluorescence intensities were scored semi-quantitatively. Very bright immunofluorescence reactivity (of intensity up to 4) on the wild-type enzyme transfected HEK293 cells with sera from the patients with anti-MAG IgM Gammopathy was observed. This reactivity completely disappeared on the GlcAT-P mutant transfected cells.

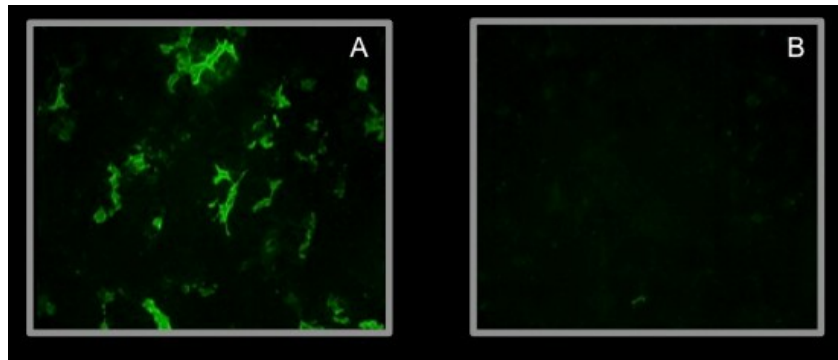


**Figure 13: Confirmation that GlcAT-P itself is not the target antigen in patients with anti-MAG IgM Gammopathy. When patients' sera were incubated on mutant GlcAT-P transfected HEK293 cells (B), there was complete loss of immunoreactivity when compared to wild-type GlcAT-P transfected cells (A). Serum dilution was at 1:10 and a FITC-conjugated goat anti-human IgM secondary antibody was used.**

It could be confirmed that while GlcAT-P is not the target antigen itself, its enzymatic activity is essential for the formation of the glycoepitope HNK-1. Together the data shown in Chapters 5.4 and 5.5 confirmed that sera from patients with anti-MAG IgM Gammopathy specifically recognize the HNK-1 glycoepitope regardless of the protein or lipid backbone. It can also be excluded that there is endogenous expression of MAG in HEK293 cells as this protein is specific to myelin forming cells.<sup>59,85</sup> Therefore, in the absence of exogenous recombinant MAG, other endogenous cellular components in the HEK293 cells are HNK-1 glycosylated by GlcAT-P.

## **5.6 Confirmation of HNK-1 glycosylation of MAG and MAG(ec)-H<sub>6</sub> in HEK293 cells**

Incubation of anti-HNK-1 IgM antibody on HEK293 cells co-transfected with both MAG and GlcAT-P indicated a positive reactivity by indirect immunofluorescence technique. However, whether MAG itself also was being HNK-1 glycosylated remained to be confirmed.

Two approaches were taken to prove that in the presence of the enzyme GlcAT-P, MAG was being HNK-1 glycosylated in HEK293 cells. In the first approach, HNK-1 glycosylated MAG was immunoprecipitated from MAG and GlcAT-P transfected HEK293 cell lysates using an anti-HNK-1 IgM antibody. Immunodetection of glycosylated MAG was done by Western Blot using HNK-1 and MAG specific antibodies. Control transfected HEK293 cell lysates (indicated by the empty vector pTriEx-1) or cells transfected only with MAG were used as controls.

In the MAG and GlcAT-P transfected cell lysate, two protein bands were detected roughly around 80 kDa and between 50 and 65 kDa. These two proteins, presumably monomeric and dimeric MAG, could be identified by both the anti-HNK-1 and the anti-MAG antibodies. This was the first indication that when MAG is co-transfected with GlcAT-P, it was being HNK-1 glycosylated in HEK293 cells. In the absence of the enzyme GlcAT-P, MAG transfected HEK cells did not express the HNK-1 glycoepitope on MAG.



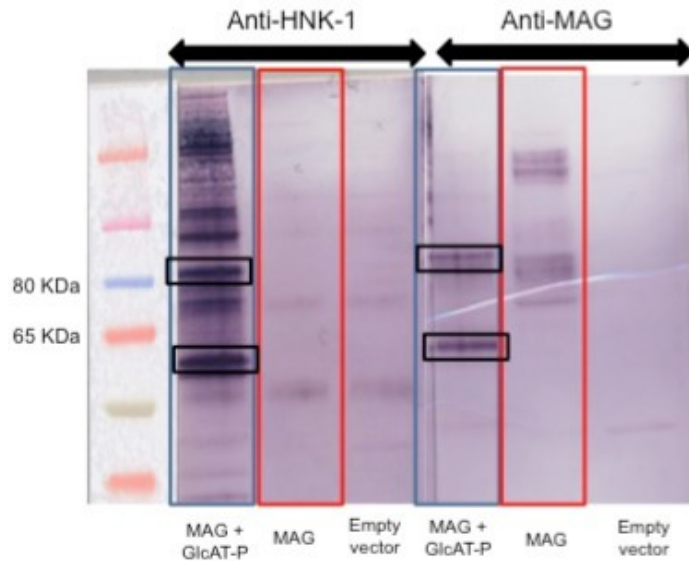


**Figure 14: HNK-1 glycosylation of MAG in the presence of GlcAT-P.** HNK-1 glycosylated MAG was identified using two different antibodies (anti-MAG mouse IgG as well as anti-HNK-1-mouse IgM) migrating at the same height (boxed in black). MAG transfected HEK293 cells do not have the HNK-1 glycosylation and was not immunoprecipitated using the anti-HNK-1 antibody. Therefore, there is no detection of MAG in the immunoprecipitated sample using the anti-MAG antibody.

In the second approach, HEK293 cells were transfected with the plasmid coding for the MAG(ec) fused with a C terminal His-tag alone (as described in Chapters 4.5, 4.7 and 5.2) or co-transfected with GlcAT-P. Western Blot analysis of the different fractions (Figure 15) using both anti-His and anti-HNK-1 antibodies proved HNK-1 modification of MAG(ec)-H<sub>6</sub>.

The HNK-1 modification increased the electrophoretic mobility of the MAG(ec)-H<sub>6</sub> despite HNK-1 glycosylated MAG being larger than non HNK-1 glycosylated MAG. This change could be attributed to the presence of the terminal sulfate group in the HNK-1 epitope increasing the overall negative charge and leading to an increased electrophoretic mobility.

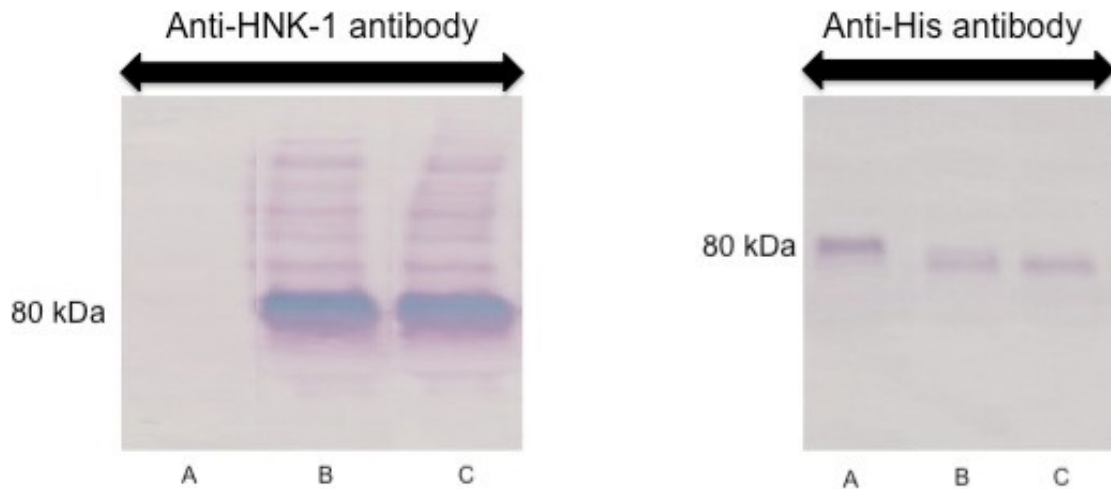


Figure 15: HNK-1 glycosylation of MAG(ec)-H<sub>6</sub>. Western blot analysis of MAG(ec)-H<sub>6</sub> either in its non HNK-1 or HNK-1 glycosylated form (co-transfection with GlcAT-P or GlcAT-P and HNK-1ST) is shown. A, B and C are labelled as HNK-1 unglycosylated MAG(ec), unglycosylated MAG(ec)+GlcAT-P and unglycosylated MAG(ec)+GlcAT-P+HNK-1ST respectively. Detection by the anti-HNK-1 mouse IgM antibody shows successful glycosylation of MAG in the presence of GlcAT-P. Anti-His antibody detection (right) indicates a difference in electrophoretic mobility between HNK-1 unglycosylated and HNK-1 glycosylated MAG.

### 5.7 IMAC purification of His-tagged MAG(ec)-H<sub>6</sub>

Having confirmed that MAG(ec)-H<sub>6</sub> in the presence of GlcAT-P in the HEK293 cell system was being HNK-1 glycosylated, in the next step HNK-1 glycosylated His-tagged MAG(ec) was isolated to be subsequently used for the ELISA development. Purification of HNK-1 glycosylated His-tagged MAG(ec) was done by IMAC using a nitrilotriacetic acid (NTA) complexed nickel<sup>2+</sup> chromatography matrix. All the chromatographic elution fractions containing the purified protein were analyzed by Western Blot using an anti-His-tag antibody.

### 5.8 No neutralization of anti-HNK-1 IgM antibody by soluble glycosylated MAG

A neutralization assay was performed using the IMAC purified variation of HNK-1 glycosylated MAG(ec)-H<sub>6</sub>, where the soluble form of the antigen was incubated either with the commercially available mouse anti-HNK-1 IgM antibody or a randomly selected serum from a patient with anti-MAG IgM Gammopathy. Both

the serum sample and the anti-HNK-1 IgM antibody was diluted up to 1:1,000,000. The anti-HNK-1 IgM antibody and the anti-MAG IgM serum sample were tested before and after the neutralization on a BIOCHIP containing GlcAT-P transfected or GlcAT-P+MAG co-transfected HEK293 cells by IIFT. No differences in the immunofluorescence reactivities between the two groups were noticed, indicating that there was no neutralization of IgM antibody by soluble HNK-1 glycosylated MAG. No neutralization was observed even at the very high serum dilutions keeping the antigen concentration constant. This indicated that the effect was not due to fewer available HNK-1 antigenic epitopes and a high concentration of the corresponding IgM antibody, but rather this is a property of the IgM molecule itself.

Table 8 is a comparison of a single randomly selected serum sample of a patient with anti-MAG IgM Gammopathy (serially diluted from 1:10 to 1:1,000,000) incubated on HEK293 cells transfected with either MAG and GlcAT-P or GlcAT-P alone. Serum sample incubation on HEK293 cell transfectants were either after the neutralization assay by soluble HNK-1 glycosylated MAG or with no prior neutralization.

**Table 8: Neutralization assay with serum and purified soluble HNK-1 glycosylated MAG(ec)-H<sub>6</sub>. The '+' indicates "after neutralization" and the '-' indicates "without neutralization".**

sample	Dilution	MAG(ec)- HNK-1- H <sub>6</sub>	MAG + GlcAT-P	GlcAT-P	Negative control
anti-MAG/HNK-1 IgM positive human serum	1:10	-			
		+			
	1:100	-			
		+			
	1:1.000	-			
		+			
	1:10.000	-			
		+			
	1:100.000	-			
		+			
	1:1.000.000	-			

## 5.9 Sequencing of variable heavy (VH) and variable light (VL) chains of anti-HNK-1-IgM mouse hybridoma

Monoclonal antibodies are a useful alternative to human blood derived antibodies to be used as a reference material. To generate a human IgM like chimeric antibody made of the HNK-1-specificity defining variable regions of the mouse anti-HNK-1-monoclonal IgM the variable sequences have to be identified.

Mouse Hybridoma ATCC TIB200, secreting an anti-HNK-1 antibody, was used for mRNA isolation and subsequent cDNA synthesis using Ig-specific oligonucleotides.

Due to the fact that 15 to 35 percent of the VH or VL sequences of murine hybridomes are not amplifiable with standard consensus primers,<sup>86</sup> 5'RACE PCR was used to clone the V domains of both the heavy and light chains that make up the HNK-1 antigen binding site of the antibody.

Used for RT PCR →→ oligo dT; TTTTTTTTTTTTTTTTTTTTTTTTTT

With dC Tailing at the 3' end of 1<sup>st</sup> strand cDNA

### ***Amplification of variable heavy (VH) sequence:***

oligo\_dG\_VH ; tat`ggctc`acatgGGGGGGGGGGGGGGGGGG  
Eco31I(NcoI)

asense CH1M\_Mm ; tat`ggctc`acgcGCCACCAGATTCTTATCAGACAGG  
Eco31I

### ***Amplification of variable light kappa (VK) sequence:***

oligo\_dG\_VL\_K ; tat`cgctc`acgcgGGGGGGGGGGGGGGGGGG  
BsmBI(MluI)

MKV.B\_Bsp ; aat`CGTCTC`gGGCCcCGGATACAGTTGGTGCAGCATC  
BsmBI

The VH and VK amplification products were digested using Eco31I and BsmBI respectively and ligated into NcoI and Bsp120I digested pTriEx-1-sp-dCH1-3G1(mhr) (EUROIMMUN, Germany).

The VH and VL cDNA were analysed with the online tool IgG-BLAST using the murine reference database. (<https://www.ncbi.nlm.nih.gov/igblast/>)

**Table 9: Summary of the Ig-BLAST of the VH and VL cDNA sequences of the mouse HNK-1.**

HNK-1				
VH			VL	
QVQLKQSGPGLVQPSQSL(SIT)TVSGFSLTS YGVHWVRQSPGKGLEWLGVIWSSGGSTDYNA AFISRLSISKDASKSQVFFKMNSLHATDTAIYY (C)ARGYGSRGDYWGQGTSVTVSS			DIQMTQSPSSLSASLGERVSLT(C)RASQDIGSS LNWLQQEPDGTIKRLIYATSSLD(S)GVPKRFSG SRSGSDYSLTISSEDFVDYY(C)LQYASFPY TFGGGTKLEIKR	
V-(D)-J junction details based on top germline gene matches:			V-(D)-J junction details based on top germline gene matches:	
V region end	V-D junction *	D region	D-J junction *	J region start
CCAGA	GG	CTACG GTAGT AG	GGG	GGACT
*: Overlapping nucleotides may exist at V-D-J junction (i.e, nucleotides that could be assigned to either rearranging gene). Such nucleotides are indicated inside a parenthesis (i.e., (TACAT)) but are not included under the V, D or J gene itself.			*: Overlapping nucleotides may exist at V-D-J junction (i.e, nucleotides that could be assigned to either rearranging gene). Such nucleotides are indicated inside a parenthesis (i.e., (TACAT)) but are not included under the V, D or J gene itself.	
Sub-region sequence details:			Sub-region sequence details:	
	Nucleotide sequence	Translation		
CDR3	GCCAGAGGCTACGGTAG TAGGGGGGACTAC	ARGYGS RGDY		
	Nucleotide sequence	Translation		
CDR3	CTACAATATGCTAGT TTTCCGTACACG	LQYASFPYT		
Alignment summary between query and top germline V gene hit:			Alignment summary between query and top germline V gene hit:	
	from	to	mismatches	identity (%)
FR1-IMGT	1	75	0	100
CDR1-	76	99	0	100
	matches	mismatches	identity (%)	
FR1-IMGT	78	0	100	
CDR1-IMGT	18	0	100	

IMGT					FR2-IMGT	51	0	100
FR2-IMGT	100	150	0	100	CDR2-IMGT	9	0	100
CDR2-IMGT	151	171	0	100	FR3-IMGT	107	1	99.1
FR3-IMGT	172	285	5	95.6	CDR3-IMGT (germline)	19	1	95
CDR3-IMGT (germline)	286	291	0	100	Total	282	2	99.3
Total			5	98.3				

The query sequence (i.e., in this case the VH and VL cDNA sequences of the mouse HNK-1) was analysed with this tool allowing to view matches to the germline V, D, J genes, the Ig variable domain framework region (FR) and the complementarity determining region (CDR) (as indicated in the table) and compared with other Ig sequences in the database. In addition to showing the detailed alignment between the query and search hits, the report includes identifying the V, D and J genes, a summary of the relationship between the coding frames of the V and J genes of the VL and the V, D, J genes for the VH domains as well as the match statistics for the various FR/CDR regions. The table indicates the correct coding sequences of the VH and VL regions of the mouse HNK-1 with conserved Cysteine residues of disulfide bonds identified (highlighted). Antibody maturation results in sequence diversification of the CDR hypervariable regions and of the Framework regions. Examination of the VH and VL sequences also indicated a high degree of similarity to the genomic sequence, suggesting a low degree of maturation.<sup>87</sup>

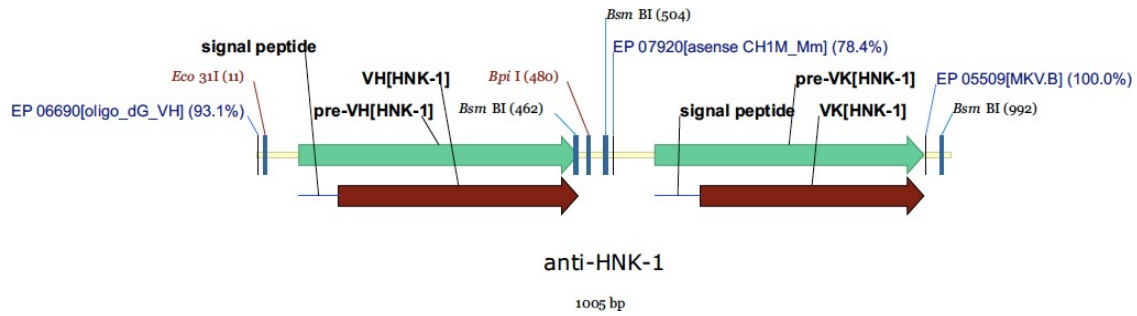


**Figure 16: Schematic presentation of the HNK-1 mouse IgM VH/VL construct.**

The correct VH/VL sequences were fused to human immunoglobulin heavy constant mu (IGHM) and immunoglobulin kappa constant (IGKC) to produce the chimeric IgM and they were analysed functionally for binding to the HNK-1 antigen.

## 5.10 Anti-MAG/HNK-1 IgM ELISA

Purified MAG(ec)-HNK-1-H<sub>6</sub> was used to set up an indirect anti-MAG IgM ELISA.

HNK-1 modified MAG(ec) (i.e., MAG(ec)-HNK-1-H<sub>6</sub>) and in parallel MAG(ec) (i.e., MAG(ec)-H<sub>6</sub>) without the modification were isolated by IMAC (Chapter 4.8) followed by ion-exchange chromatography.

Maxisorp<sup>®</sup> ELISA plates were coated with 100 ng/well of purified MAG protein preparations. Five randomly selected serum samples out of a cohort of 32 sera from patients with anti-MAG IgM Gammopathy and 10 sera from healthy blood donors as negative controls were tested at a dilution of 1:100. The anti-HNK-1 IgM antibody was used as a coating control. The optical density (OD) values at 450 nm were measured and plotted against the respective serum of the patient or healthy donor comparing between the two antigenic preparations as well as the two different types of ELISA plates.

The Maxisorp<sup>®</sup> plate gave very high OD values for every patient serum tested at 1:100 dilution. However, the samples from healthy blood donors also gave comparatively high background values. Due to the high IgM titres in these anti-



MAG IgM Gammopathy patients, higher serum dilutions could be used without reducing sensitivity while maintaining high specificity.

All serum samples from patients with anti-MAG IgM Gammopathy and healthy blood donors were further analyzed at 1:1000 dilution. The serum dilutions were tested on the HNK-1 glycosylated and non-HNK-1 glycosylated MAG(ec)-H<sub>6</sub> was used as a negative control. While OD values of sera from the patients remained comparably high at the 1:1000 dilution, the OD values from the healthy blood donors (which are the “background” signal) were significantly reduced to negligible detection on MAG(ec)-HNK-1-H<sub>6</sub> coated Maxisorp<sup>®</sup> plates.

There was variation in OD values between the different patients indicating varying titers of anti-HNK-1 IgM antibodies. There was no reactivity seen on the plate coated with HNK-1 unglycosylated MAG(ec)-H<sub>6</sub>.

### HNK-1 glycosylated MAG(ec)-H6\_dilution 1:1000

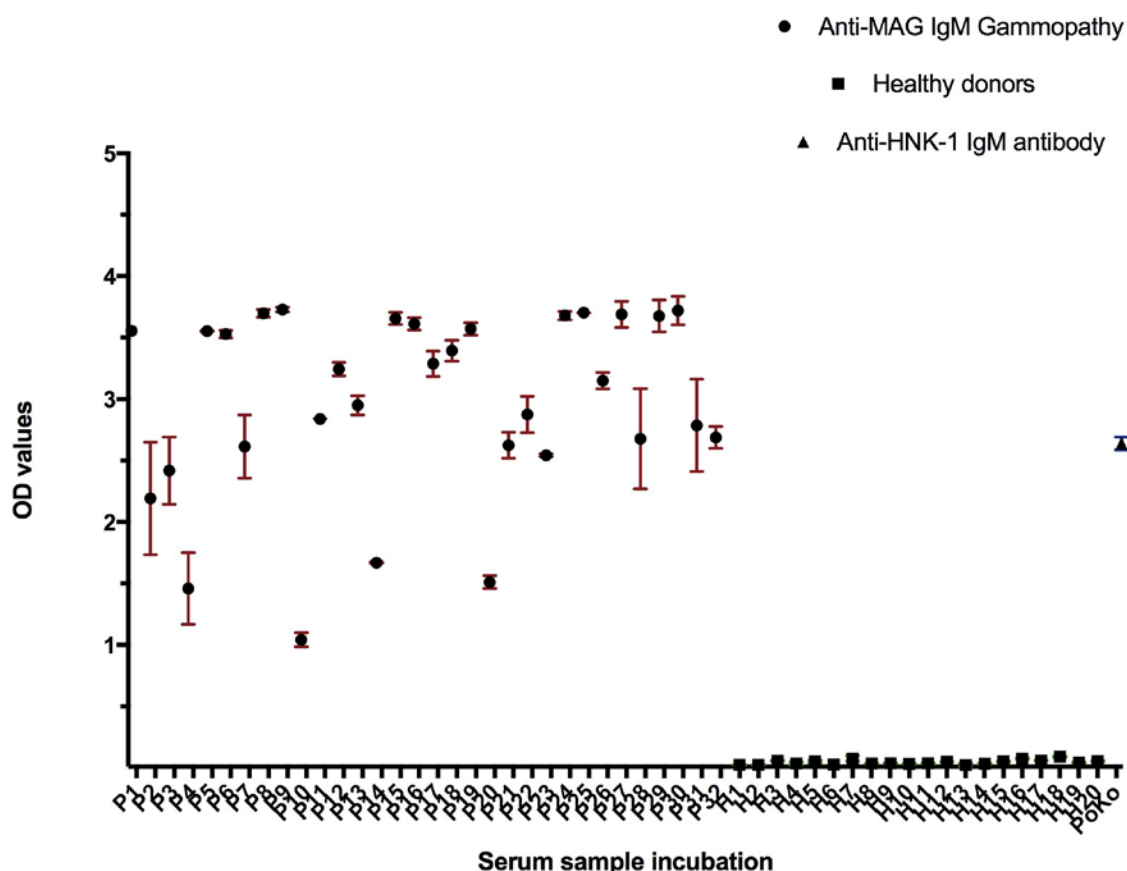


Figure 17: Comparison of OD values at 1:1000 sample dilution on HNK-1 glycosylated MAG(ec)-H<sub>6</sub> coated Maxisorp® plates. Maxisorp® plate coated with purified His-tagged HNK-1 glycosylated MAG was incubated with serum samples of 32 patients (P) with anti-MAG IgM Gammopathy and 20 healthy blood donors (H) at a dilution of 1:1000. PoKo refers to the positive control, human anti-HNK-1 IgM antibody. OD values were plotted against their sample number. All patients showed high OD values, while all sera from healthy blood donors had negligible OD values. Data are expressed as mean ± s.e.m.

Table 10 gives a comprehensive comparison of sensitivity on three different diagnostic tools available to detect anti-MAG IgM antibodies. The anti-MAG/HNK-1 ELISA is the most sensitive assay with antibody titres detectable at 1:1000 serum dilution. The cell based assay also shows a high sensitivity for all samples tested at 1:1000, with the exception of one serum sample where immunofluorescence was detected only at 1:100 dilution. On the other hand, the

typical “MAG pattern” was best observed at 1:10 dilution on monkey peripheral nerve tissue sections and only in 59 % of the patients’ sera tested.

**Table 10: Comparison between recombinant cell based assay, anti-MAG/HNK-1 ELISA and tissue sections for the detection of IgM antibodies in patients with anti-MAG IgM Gammopathy.**

<b>Serum samples</b>	<b>Monkey sural nerve (IIFT) (IgM titre)</b>	<b>HNK-1 recombinant cell based assay (IIFT) (IgM titre)</b>	<b>Anti-MAG(ec)-H<sub>6</sub> HNK-1 IgM ELISA (OD 450/620) (Serum dilution 1:1000)</b>
MAG serum 1	1:10	> 1:1000	3.6
MAG serum 2	Negative	> 1:1000	2.2
MAG serum 3	Negative	> 1:1000	2.4
MAG serum 4	Negative	> 1:1000	1.5
MAG serum 5	1:10	> 1:1000	3.6
MAG serum 6	1:10	> 1:1000	3.5
MAG serum 7	Negative	> 1:1000	2.6
MAG serum 8	1:10	> 1:1000	3.7
MAG serum 9	1:10	> 1:1000	3.7
MAG serum 10	Negative	1:100	1.0
MAG serum 11	Negative	> 1:1000	2.8
MAG serum 12	1:10	> 1:1000	3.2
MAG serum 13	1:10	> 1:1000	2.9
MAG serum 14	Negative	> 1:1000	1.7
MAG serum 15	1:10	> 1:1000	3.7
MAG serum 16	1:10	> 1:1000	3.6
MAG serum 17	1:10	> 1:1000	3.3
MAG serum 18	1:10	> 1:1000	3.4
MAG serum 19	1:10	> 1:1000	3.6
MAG serum 20	Negative	> 1:1000	1.5
MAG serum 21	Negative	> 1:1000	2.6
MAG serum 22	1:10	> 1:1000	2.9
MAG serum 23	Negative	> 1:1000	2.5
MAG serum 24	1:10	> 1:1000	3.7
MAG serum 25	1:10	> 1:1000	3.7
MAG serum 26	1:10	> 1:1000	3.1
MAG serum 27	1:10	> 1:1000	3.7
MAG serum 28	Negative	> 1:1000	2.7

MAG serum 29	1:10	> 1:1000	3.7
MAG serum 30	1:10	> 1:1000	3.7
MAG serum 31	Negative	> 1:1000	2.8
MAG serum 32	Negative	> 1:1000	2.7
Healthy donor 1	Negative	Negative	0.03
Healthy donor 2	Negative	Negative	0.03
Healthy donor 3	Negative	Negative	0.06
Healthy donor 4	Negative	Negative	0.04
Healthy donor 5	Negative	Negative	0.05
Healthy donor 6	Negative	Negative	0.03
Healthy donor 7	Negative	Negative	0.08
Healthy donor 8	Negative	Negative	0.04
Healthy donor 9	Negative	Negative	0.04
Healthy donor 10	Negative	Negative	0.03
Healthy donor 11	Negative	Negative	0.04
Healthy donor 12	Negative	Negative	0.05
Healthy donor 13	Negative	Negative	0.02
Healthy donor 14	Negative	Negative	0.03
Healthy donor 15	Negative	Negative	0.05
Healthy donor 16	Negative	Negative	0.08
Healthy donor 17	Negative	Negative	0.06
Healthy donor 18	Negative	Negative	0.09
Healthy donor 19	Negative	Negative	0.04
Healthy donor 20	Negative	Negative	0.05
Positive Control (anti-HNK-1 IgM antibody)	1:10	1:1000	2.6

## 6. Discussion

### 6.1 Ischemic stroke does not result in the induction of autoantibodies against neuronal structures

An autoimmune response as an epiphenomenon of cerebral tissue injury following a stroke has long been considered plausible. Different methods have previously been used to detect antibodies in stroke patients (Chapter 2.11), but so far only limited number of studies have addressed whether stroke induced autoantibodies bind to brain tissue sections or mammalian cells expressing recombinant neuronal antigens.<sup>54</sup>

The objective of this study was therefore to investigate the presence of stroke induced autoantibodies binding to neuronal antigens. For this purpose, autoantibody profiling of serum samples from 68 stroke patients and 21 healthy controls were done on primate and rat brain tissue sections and recombinant cell based substrates using indirect immunofluorescence technique.

Screening of the IgG, IgM and IgA repertoire of patients indicated that stroke neither results in any new autoreactivity against neuronal targets nor is there any increase in autoreactivity already prevalent in patients before the occurrence of a stroke. Further, the frequency of autoreactivity to each antigen was extremely low. Finally, the disease associated repertoire was essentially indistinguishable from that in age matched controls and finally, in all patients antibody responses to autoantigens were pre-existing.

A low intensity immunofluorescence reactivity of antibodies specific to “commonly identified antigens” like myelin components and nuclear proteins at 1:10 serum dilution were detected in the stroke patients as well as in the healthy controls. The prevalence of this baseline reactivity (the values of those that have not been recorded) can be attributed to the presence of the natural autoantibody repertoire in every individual. By definition, the presence of “natural antibodies” implies the presence of autoantibodies in the serum of healthy individuals that bind to self-antigens *in vivo*. The healthy immune system contains self-reactive B- and T-cells and natural autoantibodies reactive with self-molecules.<sup>88</sup> Therefore, it is not

surprising that low level prevalence of such autoantibodies were also detected in the patients with stroke.<sup>89</sup>

Moreover, of the autoreactivities that have been recorded, all the patients already harboured such antibodies prior to the stroke as evidenced by their presence on days 0, 1 and 90. This is another line of evidence supporting the theory that the presence of these antibodies is not a consequence of ischemic stroke.<sup>90,91</sup> A humoral immune response normally becomes effective only several days after initiation by an antigen.<sup>92,93</sup> Therefore, it seems highly unlikely that an autoimmune response to any antigen would develop within < 24 hours following stroke.

The presence and possible role of anti-NMDAR antibodies in stroke patients have been discussed controversial.<sup>54,94</sup> One of the focuses of this study was to re-address the question whether patients developed antibodies to NMDAR following stroke. None of the stroke patients harboured autoantibodies to NMDAR of the IgG isotype. IgM or IgA reactivity to NMDAR was limited to HEK293 cells transfected with the subunit NR1 and no NMDAR reactivity pattern was observed on brain tissue sections. The significance of this finding remains to be clarified as one of the more acceptable methods of anti-NMDAR antibody detection is both on rat hippocampus tissue sections in combination with recombinant cell based immunofluorescence.<sup>95</sup> Moreover, the pathological significance of these anti-NMDAR antibodies of IgA and IgM isotype also remain to be clarified.<sup>96,97, 98,99</sup> Finally, none of the stroke patients developed any signs of autoimmune encephalitis which is the corresponding disease in patients with anti-NMDAR antibodies.

Interestingly, one of the healthy controls in this study also had an IgA reactivity to NMDAR subunit NR1. This finding is in accordance with other studies by *Kalev-Zylinska et al.* which shows that the presence of antibodies to NMDAR may not be stroke specific as up to 3 % of healthy controls also harbor low levels of such antibodies.<sup>54</sup> Other studies have also confirmed the presence of anti-NMDAR antibodies in healthy controls.<sup>100,101</sup>

It is not unusual that stroke does not result in autoimmunity. It has been hypothesized that severe brain ischemia results in systemic immunodepression to prevent autoimmune reactions against exposed CNS antigens but at the same time increasing the susceptibility of such patients to life-threatening infections.<sup>102</sup> It is thought that through the autonomic nervous system (ANS) the ischemic brain exerts a potent immunosuppressive effect on lymphoid organs.<sup>42,103</sup> In human studies, a loss of function of CD4+ T cells was documented in patients who developed post-stroke infections which was associated with signs of immunosuppression.<sup>104</sup> Several groups have repeatedly shown that changes in the adaptive immunity following a stroke results in the apparent shut down of the immune system.

There are some hints suggesting the protective role of regulatory T- and B cells that can suppress CNS inflammation post ischemia. Antigen presentation following stroke can result in different outcomes including the activation of regulatory T cells which is of particular importance as it contributes to regulatory immune mechanisms. Experiments in the rodent model of stroke have shown that regulatory T cells are active players in contributing to neuroprotection by secreting interleukin 10 (IL-10) into the brain.<sup>105</sup> Since interactions between T- and B-cells are crucial in the secretion of autoantibodies to CNS antigens, the presence of regulatory T cells following a stroke may limit the development of a humoral response.<sup>106</sup> There are also groups stating the presence of regulatory B cells playing a crucial role in conferring a cytoprotective effect following stroke.<sup>43</sup> Patients with acute ischemic stroke have elevated numbers of IL-10 secreting peripheral blood mononuclear cells (PBMC) and also higher concentration of IL-10 is detected in the CSF.<sup>107</sup>

Therefore, it may be an immunomodulatory response of the adaptive immune system following a stroke or the presence of regulatory subsets of T cells and B cells or a combination of both factors that limit the development of a humoral response.<sup>108</sup>

## **6.2 Development of new diagnostic tools for the detection of anti-MAG/HNK-1 IgM antibodies**

Anti-MAG IgM Gammopathy is a rare paraproteinemia of the IgM subtype that affects the peripheral nervous system. Despite the name of the disease suggesting that these antibodies recognize the myelin associated glycoprotein, the antigenic determinant of anti-MAG IgM antibodies is essentially a terminally sulfated trisaccharide, the HNK-1 carbohydrate epitope.

One of the standard methods of detection of anti-MAG IgM antibodies is to confirm the “typical MAG pattern” (Chapter 2.19) that is seen when sera from patients with anti-MAG IgM Gammopathy are incubated on peripheral nerve sections. However, the sensitivity of this method to detect anti-MAG IgM antibodies on nerve tissue is low. This was demonstrated by incubation of serum samples from patients with anti-MAG IgM Gammopathy where only 59 % of the patients’ sera showed reactivity at 1:10 dilution while the remaining were not detected on the nerve tissue section at all. Although none of the healthy blood donors were positive for this “typical MAG pattern”, the sensitivity of the tissue sections was highly variable between the different patients with anti-MAG IgM Gammopathy.

To overcome this issue of sensitivity, a cell based assay was developed using recombinant techniques. These techniques not only allow controlled and scalable production of recombinant proteins but are also an alternative to the use of animal tissue.

The cDNAs encoding the two enzymes involved in the biosynthesis of the antigenic glycoepitope HNK-1 were cloned, as it has previously been done.<sup>61</sup> Production of recombinant HNK-1 glycosylated MAG was based on the HEK293 mammalian cell system because these cells are able to generate human proteins with their correct conformation. Recombinant expression of active GlcAT-P alone in HEK293 cells was sufficient to attach the HNK-1 carbohydrate on endogenous proteins and/or lipids on the cell surface. This may be possible because of sufficient amounts of endogenous HNK-1ST that is already present in the



HEK293 cells. Transfected cells were formalin fixed and analyzed by indirect immunofluorescence. Expression of HNK-1 was controlled with a mouse monoclonal anti-HNK-1 IgM antibody. This motif was specifically recognized by sera from patients with anti-MAG IgM Gammopathy tested at dilutions 1:10, 1:100 and 1:1000. With the exception of one patient from a cohort of 32 samples, all other sera were positive on this recombinant cell-based indirect immunofluorescence assay at 1:1000 serum dilution. However, at 1:100 dilution, all serum samples were positive on the recombinant HEK293 cells expressing the HNK-1 glycoepitope while specificity also remained at 100 %. The recombinant cell based assay can replace peripheral nerve tissue section when a sample dilution of 1:100 is used.

Although this cell based immunofluorescence assay using recombinant HNK-1 glycosylated MAG is a sensitive and specific tool, it allows only semi-quantitative detection of antibodies in patients with anti-MAG IgM Gammopathy. Since ELISAs are one of the most sensitive quantitative immunoassays available, purified HNK-1 glycosylated MAG from HEK293 cells was used to develop an anti-MAG/HNK-1 ELISA allowing the precise detection of anti-MAG IgM antibodies. Testing a cohort of 32 serum samples with a variety of antibody titres and sera from healthy blood donors, reactivity of this assay was specific to HNK-1 glycosylated MAG and only in patients that have clinically been diagnosed with anti-MAG IgM Gammopathy.

The choice of MaxiSorp® ELISA plate was based on the surface which is appropriate for immobilization of the biomolecule. While at a lower serum dilution of 1:100 there was a relatively high background caused by healthy donor samples, at a dilution of 1:1000, both the sensitivity and specificity of the assay remained at 100 % while the background reactivity given by the healthy blood donors had been further reduced to almost undetectable values.

Soluble MAG (HNK-1) was unable to neutralize the anti-HNK-1 IgM leading to the speculation that perhaps the ability of a pentameric IgM molecule to bind to its antigen is high only when the antigen is cell bound or immobilized on a

surface resulting in a multimeric state. The avidity of an antibody molecule is dependent on the multimeric state of antibody antigen interaction. In case of immobilized HNK-1 antigen, this multimeric interaction with a IgM is possible resulting in higher avidity than in the case of soluble HNK-1.

Therefore, the effective binding of an IgM molecule to its target antigen is influenced by the spatial conformation and availability of all the antigenic determinants. The higher avidity of IgM also possibly makes it highly reactive to such glyco-structures.

### **6.3 Concluding remarks**

Stroke is a prototypical example of neuroinflammation where there is uninhibited infiltration of immune cells and serum proteins across a compromised BBB into the CNS. In the course of this thesis, the focus was whether a specific biomarker in stroke patients could be identified. However, it was found that stroke does not induce autoantibodies to neuronal structures.

On the other hand, anti-MAG IgM Gammopathy is an immune mediated disease of the peripheral nervous system where autoantibodies (anti-MAG IgM) are a biomarker. In this case a range of *in vitro* recombinant DNA techniques and proteomics were used to develop powerful tools for the specific and sensitive detection of these pathogenic autoantibodies. These methodologies can be translated to other diseases where the antigen is well defined.

## Bibliography

1. Pieper, K. *et al.* B-cell biology and development. *J. Allergy Clin. Immunol.* **131**, 959–971 (2013).
2. Melchers, F. Checkpoints that control B cell development. *J. Clin. Invest.* **125**, 2203–2210 (2015).
3. Delves, P. J. *et al.* *Roitt's essential immunology*. **12th ed.**, (2011).
4. Owen, J., *et al.* *Kuby Immunology*. **6th ed.**, (2012).
5. Minges Wols, H. A. Plasma Cells. *eLS* 1–11 (2015).
6. Cambier, J. C. *et al.* B-cell anergy: from transgenic models to naturally occurring anergic B cells? *Nat. Rev. Immunol.* **7**, 633–643 (2007).
7. Rose, N. R. Molecular mimicry and clonal deletion: A fresh look. *J. Theor. Biol.* **375**, 71–76 (2015).
8. Sandel, P. C. & Monroe, J. G. Negative Selection of Immature B Cells by Receptor Editing or Deletion Is Determined by Site of Antigen Encounter. *Immunity* **10**, 289–299 (1999).
9. Allman, D. & Pillai, S. Peripheral B Cell Subsets. *Curr. Opin. Immunology* **20**, 149–157 (2008).
10. Shaffer, A. L. *et al.* Lymphoid malignancies: The dark side of B-cell differentiation. *Nat. Rev. Immunol.* **2**, 920–932 (2002).
11. Zhang, X. Regulatory functions of innate-like B cells. *Cell. Mol. Immunol.* **10**, 113–121 (2013).
12. Benson, M. J. *et al.* Affinity of antigen encounter and other early B cell signals determine B cell fate. *Curr. Opin. Immunol.* **19**, 275–280 (2007).
13. Avalos, A. M. & Ploegh, H. L. Early BCR events and antigen capture, processing, and loading on MHC class II on B cells. *Front. Immunol.* **5**, 1–5 (2014).
14. Otipoby, K. L. *et al.* The B-cell antigen receptor integrates adaptive and innate immune signals. *Proc. Natl. Acad. Sci. U. S. A.* **112**, 12145–12150 (2015).

15. Heinen, E. *et al.* The lymph follicle: a hard nut to crack. *Immunol. Today* **9**, 240–243 (1988).
16. Haji-Ghassemi, O. *et al.* Antibody recognition of carbohydrate epitopes. *Glycobiology* **25**, 920–952 (2015).
17. Alberts, B. *et al.* *Molecular Biology of the Cell*. **4th Ed.**, (2002).
18. Schroeder, H. W. J. & Cavacini, L. Structure and Function of Immunoglobulins. *J. Allergy Clin. Immunol.* **125**, 41–52 (2010).
19. Ye, J. *et al.* IgBLAST: an immunoglobulin variable domain sequence analysis tool. *Nucleic Acids Res.* **41** (2013).
20. Market, E. & Papavasiliou, F. N. V(D)J recombination and the evolution of the adaptive immune system. *PLoS Biology* **1** (2003).
21. Scofield, R. H. Autoantibodies as predictors of disease. *Lancet* **363**, 1544–1546 (2004).
22. Leslie, D. *et al.* Autoantibodies as predictors of disease. *Infect. Immun.* **108**, 1417–1422 (2001).
23. Cross, A. H. & Waubant, E. MS and the B cell controversy. *Biochim. Biophys. Acta - Mol. Basis Dis.* **1812**, 231–238 (2011).
24. Vincent, A. *et al.* Autoantibodies associated with diseases of the CNS: New developments and future challenges. *Lancet Neurol.* **10**, 759–772 (2011).
25. Zuliani, L. *et al.* Central nervous system neuronal surface antibody associated syndromes: review and guidelines for recognition. *J. Neurol. Neurosurg. Psychiatry* **83**, 638–645 (2012).
26. Hawkins, B. T. & Davis, T. P. The blood-brain barrier/neurovascular unit in health and disease. *Pharmacol. Rev.* **57**, 173–185 (2005).
27. Tietz, S. & Engelhardt, B. Brain barriers: Crosstalk between complex tight junctions and adherens junctions. *J. Cell Biol.* **209**, 493–506 (2015).
28. Rubin, L. L. & Staddon, J. M. The Cell Biology of the blood-brain-barrier. *Annu. Rev. Neurosci.* **22**, 11–28 (1999).
29. Mark, K. S. & Davis, T. P. Cerebral microvascular changes in permeability and tight junctions induced by hypoxia-reoxygenation. *Am. J. Physiol. Hear. Circ. Physiol.* **282**, 1485-1494 (2002).

30. Engelhardt, B. *et al.* The movers and shapers in immune privilege of the CNS. *Nat. Immunol.* **18**, 123–131 (2017).
31. Huang, J. *et al.* Inflammation in stroke and focal cerebral ischemia. *Surg. Neurol.* **66**, 232–245 (2006).
32. Lindsberg, P. J. & Grau, A. J. Inflammation and infections as risk factors for ischemic stroke. *Stroke* **34**, 2518–2532 (2003).
33. Wang, Q. *et al.* The inflammatory response in stroke. *J. Neuroimmunol.* **184**, 53–68 (2007).
34. Kamel, H. & Iadecola, C. Brain-immune interactions and ischemic stroke: Clinical implications. *Arch. Neurol.* **69**, 576–581 (2012).
35. Jin, R. *et al.* Inflammatory mechanisms in ischemic stroke: role of inflammatory cells. *J. Leukoc. Biol.* **87**, 779–789 (2010).
36. Magnus, T. *et al.* Immune mechanisms of stroke. *Curr. Opin. Neurol.* **25**, 334–340 (2012).
37. Lo, E. H. *et al.* Exciting, radical, suicidal: How brain cells die after stroke. *Stroke* **36**, 189–192 (2005).
38. Becker, K. J. *et al.* Autoimmune responses to the brain after stroke are associated with worse outcome. *Stroke* **42**, 2763–2769 (2011).
39. Becker, K. Autoimmune Responses to Brain Following Stroke. *Transl. Stroke Res.* **3**, 310–317 (2012).
40. Warnock, M. G. & Goodacre, J. A. Cryptic T-cell epitopes and their role in the pathogenesis of autoimmune diseases. *Br. J. Rheumatol.* **36**, 1144–50 (1997).
41. Lanzavecchia, A. How Can Cryptic Epitopes Trigger Autoimmunity? *J. Exp. Med* **181**, 1945–1948 (1995).
42. Iadecola, C. & Anrather, J. The immunology of stroke: from mechanisms to translation. *Nat Med* **17**, 796–808 (2011).
43. Chamorro, Á. *et al.* The immunology of acute stroke. *Nat. Rev. Neurol.* **8**, 401–410 (2012).
44. Dambinova, S.A. *et al.* Blood test detecting autoantibodies to N-methyl-D-aspartate neuroreceptors for evaluation of patients with transient ischemic

- attack and stroke. *Clin. Chem.* **49**, 1752–1762 (2003).
45. Becker, K. J. *et al.* Sensitization to brain antigens after stroke is augmented by lipopolysaccharide. *J Cereb Blood Flow Metab.* **25**, 1634–1644 (2005).
  46. Zhang, Z. *et al.* Human traumatic brain injury induces autoantibody response against glial fibrillary acidic protein and its breakdown products. *PLoS One* **9**, 1–16 (2014).
  47. Shibata, D. *et al.* Myelin basic protein autoantibodies, white matter disease and stroke outcome. *J. Neuroimmunol.* **252**, 106–112 (2012).
  48. Becker, K. J. Sensitization and tolerization to brain antigens in stroke. *Neuroscience* **158**, 1090–1097 (2009).
  49. Weissman, J. D. *et al.* NR2 antibodies: Risk assessment of transient ischemic attack (TIA)/stroke in patients with history of isolated and multiple cerebrovascular events. *J. Neurol. Sci.* **300**, 97–102 (2011).
  50. Bornstein, N. M. *et al.* Antibodies to brain antigens following stroke. *Neurology* **56**, 529–30 (2001).
  51. Ali, H. Y. M. & Abdullah, Z. A. Anti- $\beta$ 2-glycoprotein I autoantibody expression as a potential biomarker for strokes in patients with anti-phospholipid syndrome. *J. Immunotoxicol.* **5**, 173–177 (2008).
  52. Brey, R. L. *et al.* Antiphospholipid antibodies and stroke in young women. *Stroke* **33**, 2396–2400 (2002).
  53. Nagaraja, D. *et al.* Anticardiolipin antibodies in ischemic stroke in the young: Indian experience. *J. Neurol. Sci.* **150**, 137–142 (1997).
  54. Kalev-Zylinska, M. L. *et al.* Stroke patients develop antibodies that react with components of N-methyl-D-aspartate receptor subunit 1 in proportion to lesion size. *Stroke* **44**, 2212–2219 (2013).
  55. Bourque, P. R. *et al.* Autoimmune peripheral neuropathies. *Clin. Chim. Acta* **449**, 37–42 (2015).
  56. Kanda, T. Biology of the blood-nerve barrier and its alteration in immune mediated neuropathies. *J. Neurol. Neurosurg. Psychiatry* **84**, 208–212 (2013).
  57. Peltonen, S. *et al.* Barriers of the peripheral nerve. *Tissue barriers* **1**

- (2013).
58. Ryu, E. J. *et al.* Analysis of peripheral nerve expression profiles identifies a novel myelin glycoprotein, MP11. *J. Neurosci.* **28**, 7563–7573 (2009).
  59. Quarles, R. H. Myelin-associated glycoprotein (MAG): Past, present and beyond. *J. Neurochem.* **100**, 1431–1448 (2007).
  60. Pestronk, C. *et al.* Serum antibodies to heparan sulfate glycosaminoglycans in Guillain-Barré syndrome and other demyelinating polyneuropathies. *J. Neuroimmunol.* **91**, 204–209 (1998).
  61. Ong, E. *et al.* Biosynthesis of HNK-1 Glycans on O-linked Oligosaccharides attached to the neural cell adhesion molecule (NCAM): The requirement for core 2 $\beta$ -1, 6 N-Acetylglucosaminyltransferase and the muscle specific donamin in NCAM. *J. Biol. Chem.* **277**, 18182–18190 (2002).
  62. Kakuda, S. *et al.* Structural basis for acceptor substrate recognition of a human glucuronyltransferase, GlcAT-P, an enzyme critical in the biosynthesis of the carbohydrate epitope HNK-1. *J. Biol. Chem.* **279**, 22693–22703 (2004).
  63. Oka, S. *et al.* The N-glycan acceptor specificity of a glucuronyltransferase, GlcAT-P, associated with biosynthesis of the HNK-1 epitope. *Glycoconj. J.* **17**, 877–885 (2000).
  64. Terayama, K. *et al.* Cloning and functional expression of a novel glucuronyltransferase involved in the biosynthesis of the carbohydrate epitope HNK-1. *Proc. Natl. Acad. Sci. U. S. A.* **94**, 6093–6098 (1997).
  65. Dywer, C. A. *et al.* RPTP $\zeta$ /phosphacan is abnormally glycosylated in a model of muscle-eye-brain disease lacking functional POMGnT1. *Neuroscience* **220**, 47–61 (2012).
  66. Petratos, S. *et al.* High-titre IgM anti-sulfatide antibodies in individuals with IgM paraproteinaemia and associated peripheral neuropathy. *Immunol. Cell Biol.* **78**, 124–132 (2000).
  67. Stathopoulos, P. *et al.* Autoimmune antigenic targets at the node of Ranvier in demyelinating disorders. *Nat. Rev. Neurol.* **11**, 143–156 (2015).

68. Hamada, Y. *et al.* Binding specificity of anti-HNK-1 IgM M-protein in anti-MAG neuropathy: Possible clinical relevance. *Neurosci. Res.* **91**, 63–68 (2015).
69. Spagnol, G. *et al.* Expression of glycosylated recombinant human myelin-associated glycoprotein on a neuroblastoma cell line and its reactivity with HNK-1 but not human anti-MAG antibodies. *Neurosci. Lett.* **246**, 157–160 (1998).
70. Willison, H. J. & Yuki, N. Peripheral neuropathies and anti-glycolipid antibodies. *Brain* **125**, 2591–2625 (2002).
71. Dalakas, M. C. Pathogenesis and Treatment of Anti-MAG Neuropathy. *Curr. Treat. Options Neurol.* **12**, 71–83 (2010).
72. Lehmann, H. C. *et al.* Central nervous system involvement in patients with monoclonal gammopathy and polyneuropathy. *Eur. J. Neurol.* **17**, 1075–1081 (2010).
73. Hampel, H. *et al.* Short communication CNS demyelination in monoclonal gammopathy of undetermined significance (MGUS): possible cause of a dementia syndrome. 46–49 (1996).
74. Herrendorff, R. *et al.* Selective *in vivo* removal of pathogenic anti-MAG autoantibodies, an antigen-specific treatment option for anti-MAG neuropathy. *Proc. Natl. Acad. Sci. U. S. A.* **114**, 3689–3698 (2017).
75. Weiss, M. D. *et al.* Variability in the binding of anti-MAG and anti-SGPG antibodies to target antigens in demyelinating neuropathy and IgM paraproteinemia. *J. Neuroimmunol.* **95**, 174–184 (1999).
76. Ariga, T. The role of sulfoglucuronosyl glycosphingolipids in the pathogenesis of monoclonal IgM paraproteinemia and peripheral neuropathy. *Proc. Jpn. Acad. Ser. B. Phys. Biol. Sci.* **87**, 386–404 (2011).
77. Ariga, T. *et al.* Characterization of sulfated glucuronic acid containing glycolipids reacting with IgM M-proteins in patients with neuropathy. *J. Biol. Chem.* **262**, 848–853 (1987).
78. Magy, L. *et al.* Heterogeneity of Polyneuropathy Associated with Anti-MAG Antibodies. *J. Immunol. Res.* **2015**, (2015).



79. Kuijf, M. L. *et al.* Detection of anti-MAG antibodies in polyneuropathy associated with IgM monoclonal gammopathy. *Neurology* **73**, 688–695 (2009).
80. Stöcker, W. Processes and devices for examinations on immobilized biological material. Patent no. EP 0117262 (1984).
81. Jarius, S. *et al.* Standardized method for the detection of antibodies to aquaporin-4 based on a highly sensitive immunofluorescence assay employing recombinant target antigen. *J. Neurol. Sci.* **291**, 52–56 (2010).
82. Dähnrich, C. *et al.* Development of a standardized ELISA for the determination of autoantibodies against human M-type phospholipase A2 receptor in primary membranous nephropathy. *Clin. Chim. Acta* **421**, 213–218 (2013).
83. Kizuka, Y. *et al.* Distinct Transport and Intracellular Activities of Two GlcAT-P Isoforms. *J. Biol. Chem.* **284**, 9247–9256 (2009).
84. Ohtsubo, T.S. *et al.* Studies on the structure function relationship of the HNK-1 associated Glucuronyltransferase, GlcAT-P, by computer modeling and site-directed mutagenesis. *Journal of Biochemistry*, **128**, 283 - 91 (2000).
85. Owens, G. C. *et al.* Expression of recombinant myelin-associated glycoprotein in primary Schwann cells promotes the initial investment of axons by myelinating Schwann cells. *J. Cell Biol.* **111**, 1171–1182 (1990).
86. Toleikis, L. *et al.* Cloning single-chain antibody fragments (scFv) from hybridoma cells. *Methods Mol. Med.* **94**, 447–458 (2004).
87. Georgiou, G. *et al.* The promise and challenge of high-throughput sequencing of the antibody repertoire. *Nat. Biotechnol.* **32**, 158–168 (2014).
88. Quintana, F. J. & Cohen, I. R. The natural autoantibody repertoire and autoimmune disease. *Biomed. Pharmacother.* **58**, 276–281 (2004).
89. Dahm, L. *et al.* Seroprevalence of autoantibodies against brain antigens in health and disease. *Ann. Neurol.* **76**, 82–94 (2014).
90. Pisetsky, D. S. Antinuclear antibodies in healthy people: the tip of

- autoimmunity's iceberg? *Arthritis Res. Ther.* **13**, 109 (2011).
91. Prüßmann, J. *et al.* Co-occurrence of autoantibodies in healthy blood donors. *Exp. Dermatol.* **23**, 519–521 (2014).
  92. Janeway, C. A. *et al.* Immunobiology: The Immune System In Health And Disease. *Immunobiology* **5th Ed.** (2001).
  93. Pape, K. A. *et al.* The Humoral Immune Response Is Initiated in Lymph Nodes by B Cells that Acquire Soluble Antigen Directly in the Follicles. *Immunity* **26**, 491–502 (2007).
  94. Bokesch, P. M. *et al.* NMDA receptor antibodies predict adverse neurological outcome after cardiac surgery in high-risk patients. *Stroke.* **37**, 1432–1436 (2006).
  95. Dalmau, J. *et al.* Paraneoplastic anti-N-methyl-D-aspartate receptor encephalitis associated with ovarian teratoma. *Ann. Neurol.* **61**, 25–36 (2007).
  96. Lancaster, E. *et al.* Immunoglobulin G antibodies to the N-methyl-D-aspartate receptor are distinct from immunoglobulin A and immunoglobulin M responses. *Ann. Neurol.* **77**, 183 (2015).
  97. Dalmau, J. *et al.* Anti-NMDA-receptor encephalitis: case series and analysis of the effects of antibodies. *Lancet Neurol.* **7**, 1091–1098 (2008).
  98. Titulaer, M. J. *et al.* Treatment and prognostic factors for long-term outcome in patients with anti-NMDA receptor encephalitis: an observational cohort study. *Lancet Neurol.* **12**, 157–165 (2013).
  99. Peery, H. E. *et al.* Anti-NMDA receptor encephalitis. The disorder, the diagnosis and the immunobiology. *Autoimmunity Reviews* **11**, 863–872 (2012).
  100. Steiner, J. Prevalence of N-Methyl-D-Aspartate Receptor Autoantibodies in the Peripheral Blood: Healthy Control Samples Revisited. *JAMA psychiatry* **71**, 838–839 (2014).
  101. Hammer, C. *et al.* Neuropsychiatric disease relevance of circulating anti-NMDA receptor autoantibodies depends on blood–brain barrier integrity. *Mol. Psychiatry* **19**, 1143–1149 (2013).

102. Liesz, A. *et al.* Regulatory T cells are key cerebroprotective immunomodulators in acute experimental stroke. *Nat. Med.* **15**, 192–199 (2009).
103. Cui, H. *et al.* Oxidative stress, mitochondrial dysfunction, and aging. *J. Signal Transduct.* **2012** (2012).
104. Worthmann, H. *et al.* Linking infection and inflammation in acute ischemic stroke. *Ann. N. Y. Acad. Sci.* **1207**, 116–122 (2010).
105. Stubbe, T. *et al.* Regulatory T cells accumulate and proliferate in the ischemic hemisphere for up to 30 days after MCAO. *J. Cereb. Blood Flow Metab.* **33**, 37–47 (2013).
106. Chen, S. *et al.* Regulatory T cell in stroke: a new paradigm for immune regulation. *Clin. Dev. Immunol.* **2013** (2013).
107. Bodhankar, S. *et al.* IL-10-producing B-cells limit CNS inflammation and infarct volume in experimental stroke. *Metab. Brain Dis.* **28**, 375–386 (2013).
108. Planas, A. M. & Chamorro, A. Regulatory T cells protect the brain after stroke. *Nat. Med.* **15**, 138–139 (2009).

## List of Figures

<b>Figure Number</b>	<b>Figure Title</b>	<b>Page Number</b>
Figure 1	V(D)J recombination within a B cell receptor	9
Figure 2	The blood-brain barrier	11
Figure 3	Immunology of a stroke response	14
Figure 4	The anatomical compartments of a peripheral nerve	17
Figure 5	Formation of the HNK-1 glycoepitope	19
Figure 6	“Typical MAG” reactivity seen on peripheral nerve	23
Figure 7	A schematic representation of the immunoprecipitation protocol	35
Figure 8A	Cartoon of fragment (ZF1) of GlcAT-P(E284A)	44
Figure 8B	Cartoon of fragment (ZF2) of GlcAT-P(E284A)	
Figure 9	Overview of the expression construct for full length human MAG	45
Figure 10	Overview of the expression construct for MAG(ec)	45
Figure 11	GlcAT-P alone has to be supplemented to generate MAG-independent HNK-1-glycoepitope in HEK293 cells	47
Figure 12	Confirmation of these antigenic target of “anti-MAG antibodies” in patients with anti-MAG IgM Gammopathy	48
Figure 13	Confirmation that GlcAT-P itself is not the target antigen in patients with anti-MAG IgM Gammopathy	49
Figure 14	HNK-1 glycosylation of MAG in the presence of GlcAT-P	51
Figure 15	HNK-1 glycosylation of MAG(ec)-H <sub>6</sub>	52
Figure 16	Schematic presentation of the HNK-1 mouse IgM VH/VL construct	58
Figure 17	Comparison of OD values in 1:1000 sample dilution on HNK-1 glycosylated MAG(ec)-H <sub>6</sub> coated Maxisorp® plates	60

## List of Tables

<b>Table Number</b>	<b>Table Title</b>	<b>Page Number</b>
Table 1	Summary of differences between IgG and IgM	8
Table 2	List of expression plasmids and the corresponding proteins expressed	29
Table 3	List of cDNAs used for the expression of the different proteins	29
Table 4	The primers and their respective sequences that were used for the construction of the different expression constructs	30
Table 5	Summary of the cloning strategy for GlcAT-P and HNK-1ST	42
Table 6	Comparison of amino acid sequences between the wildtype and mutant GlcAT-P	44
Table 7	HNK-1 antigen BIOCHIP Mosaic	46
Table 8	Neutralization assay with serum and purified soluble HNK-1 glycosylated MAG(ec)-H <sub>6</sub>	54
Table 9	Summary of the Ig-BLAST of the VH and VL cDNA sequences of the mouse HNK-1	56-57
Table 10	Comparison between recombinant cell based assay, anti-MAG/HNK-1 ELISA and tissue sections for the detection of IgM antibodies in patients with anti-MAG IgM Gammopathy	61-62

## List of abbreviations

<b>Abbreviation</b>	<b>Full form</b>
Anti-His antibody	Anti-Histidine antibody
CNS	Central Nervous System
ELISA	Enzyme linked immunosorbent assay
GlcAT-P	Glucuronyltransferase
HEK293 cells	Human embryonic kidney -293 cells
HNK-1	Human natural killer-1
HNK-1ST	HNK-1 sulfotransferase
IIFT	Indirect immunofluorescence test
IEX	Ion-exchange chromatography
IgG/IgM	Immunoglobulin-G/ Immunoglobulin-M
IGHM/IGKC	Immunoglobulin heavy constant mu/ Immunoglobulin kappa constant
IMAC	Immobilized metal affinity chromatography
MAG	Myelin associated glycoprotein
MAG(ec)-HNK-1-H <sub>6</sub>	MAG( <b>e</b> xtracellu <b>l</b> ar domain)-HNK-1-Histidine tag
NMDAR	N-methyl-D-aspartate receptor
OD	Optical density
PNS	Peripheral Nervous System
VH/VL chain	Variable heavy/ Variable light chain

## Acknowledgements

As an Early Stage Researcher (ESR) in the Marie Curie Initial Training Network (ITN) “*nEUROinflammation*”, my entire PhD work was funded and supported by the EU FP7. I want to thank Prof. Dr. med. Markus Schwaninger and Ms. Susanne Zimmermeier for coordinating this network and for arranging all the useful workshops, intriguing lectures and the yearly meetings.

I want to thank EUROIMMUN AG, Prof. Dr. med. Winfried Stöcker, for giving me this opportunity to do my PhD work in this company and for providing all the resources and necessary support. I would like to extend my sincere thanks to my *Doktorvater* Prof. Dr. med. Ralf Ludwig for accepting me as his PhD student. I am indebted to my supervisor Dr. Christian Probst for his guidance and encouragement throughout my thesis. I am also thankful to my co-supervisor Dr. Lars Komorowski for his valuable suggestions and input in my experimental work. This work would not have been successful without the cooperation, assistance and mentoring of all the members of the Molecular Biology and Immunobiochemistry departments. I would especially like to thank Christiane B., Christiane R., Nora, Inga, Swantje, Olaf and Susann. Thank you to everyone in the laboratory in Dassow where I performed most of my experiments! There were several more departments and people involved and I want to extend my sincere gratitude to each and everyone of them who I’ve had the opportunity to interact with over the last few years. A very special thank you to Jana for being very supportive for the last few hectic months! And Ishu, my only other “culturally close” friend who has constantly been there. Also being a part of the GRK1727, I want to thank Prof. Dr. med. Detlef Zillikens for accepting me as a student in the Graduate School and all the other members for providing the “academic side” to my PhD. I especially would like to thank PD Dr. vet. Jennifer Hundt for patiently answering to all those million emails and questions that I had!

I would like to thank our collaborators for their part in my PhD research from samples to suggestions (Dr. Anna Planas, Barcelona; and especially Prof. Chris Linington, Glasgow – a huge thank you for our countless discussions on neuroimmunology over the last five years that has led me to where I am now!)

I would also like to mention Prof. Britta Engelhardt for being an inspiration and a role model to me.

Thank you ma and papa for standing by me no matter what and thank you to my “new” family in Germany – I have never felt more wanted! And to the most important and loved person in my life, my best friend and my fiancé, Philip – you have endured more than anyone else has and chose to remain!